Memoirs of Museum Victoria 74: 151–171 (2016) Published 2016

ISSN 1447-2546 (Print) 1447-2554 (On-line)
http://museumvictoria.com.au/about/books-and-journals/journals/memoirs-of-museum-victoria/

Going underground: postcranial morphology of the early Miocene marsupial mole *Naraboryctes philcreaseri* and the evolution of fossoriality in notoryctemorphians

Robin M. D. Beck[1,*], Natalie M. Warburton[2], Michael Archer[3], Suzanne J. Hand[4], and Kenneth P. Aplin[5]

[1] School of Environment & Life Sciences, Peel Building, University of Salford, Salford M5 4WT, UK and School of Biological, Earth and Environmental Sciences, University of New South Wales, Sydney, NSW 2052, Australia (R.M.D.Beck@salford.ac.uk)
[2] School of Veterinary and Life Sciences, Murdoch University, 90 South Street, Murdoch, WA 6150, Australia (N.Warburton@murdoch.edu.au)
[3] School of Biological, Earth and Environmental Sciences, University of New South Wales, Sydney, NSW 2052, Australia (m.archer@unsw.edu.au)
[4] School of Biological, Earth and Environmental Sciences, University of New South Wales, Sydney, NSW 2052, Australia (s.hand@unsw.edu.au)
[5] National Museum of Natural History, Division of Mammals, Smithsonian Institution, Washington, DC 20013-7012, USA (aplink@si.edu)
* To whom correspondence should be addressed. E-mail: R.M.D.Beck@salford.ac.uk

Abstract

Beck, R.M.D., Warburton, N.M., Archer, M., Hand, S.J. and Aplin, K.P. 2016. Going underground: postcranial morphology of the early Miocene marsupial mole *Naraboryctes philcreaseri* and the evolution of fossoriality in notoryctemorphians. *Memoirs of Museum Victoria* 74: 151–171.

We present the first detailed descriptions of postcranial elements of the fossil marsupial mole *Naraboryctes philcreaseri* (Marsupialia: Notoryctemorphia), from early Miocene freshwater limestone deposits in the Riversleigh World Heritage Area, northwestern Queensland. Qualitative functional analysis of these elements suggest that *Na. philcreaseri* was very well-adapted for burrowing, albeit somewhat less so than the living marsupial moles *Notoryctes typhlops* and *N. caurinus*. Quadratic discriminant analysis of limb measurements suggests that *Na. philcreaseri* was subterranean, and its Index of Fossorial Ability is almost identical to that of *Notoryctes* species, being among the highest known for any mammal. These results suggest that notoryctemorphians evolved their specialised, "mole-like" subterranean lifestyle prior to the early Miocene. Given that forested environments predominated in Australia until the middle-late Miocene, this transition to subterranean behaviour may have occurred via burrowing in forest floors, in which case fossorial mammals that live in tropical rainforests today (such as the placental golden moles *Chrysospalax trevelyani* and *Huetia leucorhina*) may represent reasonable living analogues for early notoryctemorphians. However, alternative scenarios, such as a cave-dwelling or semi-aquatic ancestry, should be considered. Phylogenetic analysis using a Bayesian total evidence dating approach places *Naraboryctes* as sister to *Notoryctes* with strong support (Bayesian posterior probability = 0.91), and indicates that *Naraboryctes* and *Notoryctes* diverged 30.3 MYA (95% HPD: 17.7–46.3 MYA). The age and known morphology of *Na. philcreaseri* does not preclude its being ancestral to *Notoryctes*. Using estimates of divergence times and ratios of nonsynonymous to synonymous substitutions per site, we infer that the nuclear gene "Retinol-binding protein 3, interstitial" (*RBP3*), which plays a key role in vision, became inactive in the *Notoryctes* lineage ~5.4 MYA (95% HPD: 4.5–6.3 MYA). This is much younger than previous published estimates, and postdates considerably the age of *Na. philcreaseri*, implying that *RBP3* was active in this fossil taxon; hence, *Na. philcreaseri* may have retained a functional visual system. Our estimate for the inactivation of *RBP3* in the *Notoryctes* lineage coincides with palaeobotanical evidence for a major increase in the abundance of grasses in Australia, which may indicate the appearance of more open environments, and hence selection pressure on notoryctemorphians to spend less time on the surface, leading to relaxed selection on *RBP3*. Ultimately, however, a fuller understanding of the origin and evolution of notoryctemorphians – including when and why they became "mole-like" – will require improvements in the Palaeogene fossil record of mammals in Australia.

Keywords

marsupial moles; *Notoryctes*; *Naraboryctes*; Notoryctemorphia; fossorial; subterranean; postcranial; functional morphology; marsupial phylogeny; Riversleigh; Miocene; *RBP3*; *IRBP*

"Some people might say my life is in a rut,
But I'm quite happy with what I got"
Going Underground – The Jam

Introduction

The two living species of marsupial mole – *Notoryctes typhlops* (the Southern Marsupial Mole, or Itjaritjari) and *Notoryctes caurinus* (the Northern or Northwestern Marsupial Mole, or Kakarratul) – are remarkably specialised, subterranean mammals that live in the western deserts of continental Australia (Johnson and Walton, 1989; Benshemesh and Johnson, 2003; Benshemesh, 2008; Benshemesh and Aplin, 2008). The only extant representatives of the order Notoryctemorphia (Kirsch, 1977; Aplin and Archer, 1987), both species show extreme anatomical adaptations for burrowing, including a heavily fused and conical skull, loss of external ears and functional eyes, and a postcranial skeleton that is highly modified for parasagittal scratch-digging (Stirling, 1891; Carlsson, 1904; Sweet, 1906; Johnson and Walton, 1989; Warburton, 2006). One striking molecular feature of *Notoryctes* is also probably related to its subterranean lifestyle: the gene "Retinol-binding protein 3, interstitial" (*RBP3*, often referred to as "interphotoreceptor retinoid binding protein", or *IRBP*) of *N. typhlops* is non-functional, exhibiting both frameshift mutations and premature stop codons (Springer et al., 1997; Emerling and Springer, 2014). *RBP3* plays a key role in visual pigment regeneration (Pepperberg et al., 1993), and loss of function of this gene in *N. typhlops* is presumably related to its degenerate visual system: its eyes are tiny, lack lenses and are covered by skin, and the optic nerve is absent (Stirling, 1891; Sweet, 1906). The visual system of *N. caurinus* is similarly degenerate (Benshemesh and Aplin, 2008), but to date *RBP3* has not been sequenced for this species. *RBP3* has also been shown to be pseudogenic in some subterranean rodents (Kim et al., 2011: table 2; Emerling and Springer, 2014) and in several echolocating bat species (Shen et al., 2013); as in *Notoryctes*, vision is probably of limited importance in these species, and hence selection to maintain a functional copy of *RBP3* has presumably been relaxed (Kim et al., 2011; Shen et al., 2013; Emerling and Springer, 2014).

Both *Notoryctes* species spend the vast majority of their time below ground, surfacing only rarely (Johnson and Walton, 1989; Benshemesh and Johnson, 2003; Dennis, 2004; Benshemesh, 2008; Benshemesh and Aplin, 2008); because of this, many basic aspects of their ecology and life history are unknown. Fundamental questions regarding the evolutionary history of notoryctemorphians also remain unanswered. Resolution of their phylogenetic relationships has proven difficult due to their numerous morphological autapomorphies, lack of obvious close living relatives and, until recently, complete absence of a fossil record. Indeed, some studies have even questioned whether they are marsupials (Stirling, 1888; Cope, 1892; Turnbull, 1971). However, there is now overwhelming evidence that *Notoryctes* is indeed a marsupial (e.g. Horovitz and Sánchez-Villagra, 2003; Asher et al., 2004; Nilsson et al., 2004, 2010; Beck, 2008; Beck et al., 2008; Meredith et al., 2008, 2009b, 2011; Mitchell et al., 2014). Recent phylogenetic analyses, particularly those based on molecular data (e.g. Nilsson et al., 2004, 2010; Beck, 2008; Meredith et al., 2008, 2009b, 2011; Mitchell et al., 2014), typically place *Notoryctes* in a clade with the Australian marsupial orders Dasyuromorphia (predominantly carnivorous forms such as quolls, thylacines and the numbat) and Peramelemorphia (bandicoots and bilbies); Beck et al. (2014) named this clade Agreodontia. However, the precise branching relationship between Notoryctemorphia, Dasyuromorphia and Peramelemorphia is uncertain. The previous lack of fossil evidence has also meant that the underlying factors driving the evolution of the extreme fossorial adaptations of *Notoryctes*, and the timing of when they arose, remain enigmatic.

Crucial information regarding the evolutionary history of Notoryctemorphia is now being provided with the discovery of cranial and postcranial remains of the first known fossil member of the order, *Naraboryctes philcreaseri*, from early Miocene freshwater limestone deposits at Riversleigh (Gott, 1988; Warburton, 2003; Archer et al., 2011). *Na. philcreaseri* provides the first hard evidence showing how the zalambdodont molar dentition of *Notoryctes* evolved, namely via suppression of the paracone (Archer et al., 2011). In addition, postcranial elements tentatively referred to *Na. philcreaseri* show apparent fossorial specialisations, albeit not as extreme as in *Notoryctes* species (Warburton, 2003; Archer et al., 2011). The presence of these features in *Na. philcreaseri* is perhaps surprising because available evidence suggests that Riversleigh was a rainforest environment during the early Miocene (Travouillon et al., 2009; Archer et al., 2011; Bates et al., 2014). It had previously been suggested that notoryctemorphians acquired their fossorial adaptations in a desert milieu (Archer, 1984), but there is no evidence of deserts anywhere in Australia prior to the Pleistocene (McLaren and Wallace, 2010), nor extensive grasslands prior to the middle Pliocene (Martin and McMinn, 1994; Martin, 2006; Strömberg, 2011; Black et al., 2012). The discovery of *Na. philcreaseri* has led to an alternative hypothesis, namely that these adaptations evolved for burrowing through soft rainforest floors (Archer et al., 1994; Archer et al., 2011). In support of this, analogies have been drawn with the morphologically similar but unrelated placental chrysochlorids (golden moles) of sub-Saharan Africa (Archer et al., 1994), as some extant chrysochlorid species (e.g. *Chrysospalax trevelyani*, *Huetia leucorhina*) occur in wet forest environments (Bronner, 2013).

In this paper, we present the first detailed descriptions of the postcranial skeleton of *Naraboryctes philcreaseri*, including bones not discussed by Archer et al. (2011). We present a qualitative functional interpretation of its postcranial morphology, focusing on evidence for fossoriality, and test this within a quantitative framework using multivariate discriminant analysis (see Hopkins and Davis, 2009). We also calculate the widely-used Index of Fossorial Ability (Vizcaino et al., 1999; Vizcaino and Milne, 2002) for *Na. philcreaseri* and compare it to values for *Notoryctes typhlops* and for other burrowing mammals. We discuss the changes required to derive the postcranial morphology seen in *Notoryctes* species from that seen in *Na. philcreaseri*. We present the first phylogenetic

analyses to include *Naraboryctes*, using a dated Bayesian total evidence dating approach (Ronquist et al., 2012a), the first time this method has been applied to marsupials. Finally, we use the divergence dates from our phylogenetic analysis and estimates of non-synonymous to synonymous substitution ratios to estimate the timing of inactivation of the *RBP3* gene in the notoryctemorphian lineage (Chou et al., 2002; Zhang et al., 2008), and discuss its implications for our understanding of the ecology of *Na. philcreaseri*.

In 1971, Tom and Pat Rich undertook their first fieldwork in Australia, working with the American Museum of Natural History's Dick Tedford, and using "conventional" fossil collecting methods (Archer and Hand, 1984). In 1984, however, Tom, Pat and a team of brave volunteers turned to tunnelling as a way to obtain fossils from Dinosaur Cove, on the south coast of Victoria. This was apparently the first time that a tunnel had ever been dug solely to find fossils, and over the following ten years it proved a remarkable success, albeit one requiring immense efforts in terms of time and manpower. Tom has gone on to use a similar tunnelling approach in Late Cretaceous deposits in Alaska. We think, therefore, that a paper on the evolution of burrowing in marsupial moles is particularly appropriate for this volume celebrating Tom's long and productive career and his extraordinary contribution to Australian palaeontology.

Materials and methods

As with most other vertebrate specimens collected from fossil deposits in the Riversleigh World Heritage Area, the material of *Naraboryctes philcreaseri* described here was obtained by processing limestone blocks with 5–10% acetic acid, and subsequent microscope-assisted sorting of the concentrate. None of the postcranial elements were found in direct association with dental specimens of *Na. philcreaseri*; referral is based on compatible size and presence of apparent fossorial adaptations, particularly features that closely resemble the morphology seen in *Notoryctes*. It is possible that some or all of these elements in fact belong to a different taxon, but we consider this unlikely: no mammalian group present at Riversleigh besides Notoryctemorphia is known to have either living or fossil members that show extreme specialisations for digging. Nevertheless, as with all specimens not found in direct association, these referrals should be considered tentative. All known specimens of *Na. philcreaseri* are from Riversleigh Faunal Zone B sites, which have been interpreted to be early Miocene in age based on biostratigraphy (Archer et al., 1997; Archer et al., 2006; Travouillon et al., 2006), an age assignment that is now being validated by radiometric dating (Woodhead et al., 2014). A full list of *Na. philcreaseri* postcranial specimens is given in supplementary information; they are registered in the fossil vertebrate collection of the Queensland Museum (prefix QM F).

Description and functional interpretation of the postcranial morphology of *Na. philcreaseri* follows previous studies of fossorial and subterranean mammals, both living and fossil (e.g. Stirling, 1891; Thompson and Hillier, 1905; Chapman, 1919; Campbell, 1939; Orcutt, 1940; Reed, 1951; Lehmann, 1963; Puttick and Jarvis, 1977; Rose and Emry, 1983; Gasc et al., 1986; Lessa, 1990; Stein, 1993; Warburton, 2006), as well as more general studies of mammalian morphology (e.g. Coues, 1872; Barbour, 1963; Davis, 1964; Schaller, 1992; Evans, 1993). We consider mammals to be "fossorial" if they engage in regular burrowing activities below ground but nevertheless spend considerable periods of time above ground, and "subterranean" if they spend the clear majority of their time below ground (Nevo, 1999: character 2; Lessa et al., 2008); under this definition, both living *Notoryctes* species are subterranean. Measurements for *Na. philcreaseri* were taken from complete adult specimens, where available, while measurements for *N. caurinus* and *N. typhlops* were taken from Warburton (2003: Appendix 1) and an additional *N. typhlops* specimen (SAM M637).

To quantitatively test whether the known morphology of *Na. philcreaseri* supports its interpretation as a fossorial or subterranean mammal, we used a quadratic discriminant analysis based on the "limbs only" dataset of Hopkins and Davis (2009). This dataset comprises four measurements from the humerus, two from the ulna, and two from the femur, for 115 extant subterranean, fossorial and non-burrowing mammal species (including placentals, marsupials and monotremes; see Hopkins and Davis, 2009 for full details). Hopkins and Davis (2009) found this dataset to be 86.1% accurate at distinguishing burrowing (= subterranean + fossorial) and non-burrowing taxa, and 85.2% accurate for distinguishing subterranean, fossorial and non-burrowing taxa. Hopkins and Davis (2009) estimated measurements for *Notoryctes typhlops* from published images; we have replaced these with measurements taken directly from *N. typhlops* specimen SAM M637. We added a further three modern marsupial taxa to the Hopkins and Davis (2009) dataset, namely the non-burrowing dasyurid *Dasyurus viverrinus*, the non-burrowing peramelemorphians *Isoodon macrourus*, *I. obesulus* and *Perameles gunnii*, and the fossorial peramelemorphian *Macrotis lagotis*. *Na. philcreaseri* was then added, with measurements taken from the most complete specimens and with its fossorial ability treated as unknown. Measurements for these additional taxa are given in supplementary information. The quadratic discriminant analysis was implemented in JMP, assuming equal prior probabilities for the different locomotor modes, and a plot of the first two canonical axes was produced, following Hopkins and Davis (2009: fig. 3).

To further quantify the likely fossorial ability of *Na. philcreaseri*, we compared its Index of Fossorial Ability (IFA; sometimes referred to as Olecranon Length Index) – a commonly used metric that is strongly correlated with the degree of fossoriality in various groups of mammals (Vassallo, 1998; Vizcaino et al., 1999; Elissamburu and Vizcaíno, 2004; Lagaria and Youlatos, 2006; Warburton et al., 2013; Woodman and Gaffney, 2014) – with that of *Notoryctes* and other fossorial and subterranean mammals (table 1). We calculated IFA as (olecranon length/(total ulnar length-olecranon length))*100, following Vizcaino and Milne (2002). Olecranon length was measured to the distal margin of the trochlear notch, as in Hopkins and Davis (2009; see also comments by Woodman and Gaffney, 2014: table 1). For *Na. philcreaseri*

Table 1. Selected Recent and fossil mammals with an Index of Fossorial Ability (IFA) greater than 60. Identification of Recent taxa as subterranean, fossorial or non-burrowing follows Hopkins and Davis (2009). Fossil taxa are indicated by †, and their burrowing behaviour is treated as unknown. All measurements are taken from Hopkins and Davis (2009) except those for *Naraboryctes philcreaseri* (which were taken from QM F57706; see Figs. 4a, c, e) and *Notoryctes typhlops* (which were taken from SAM M637; see Figs. 4b, d, f). IFA is calculated as (olecranon length/(total ulnar length-olecranon length))*100, following Vizcaino and Milne (2002). IFA for *Na. philcreaseri* is likely a slight overestimate, as QM F57706 is missing the distal epiphysis (see Figs. 4a, c, e), and hence total ulnar length is slightly too short; the true value is probably the same as or slightly less than that for *N. typhlops*.

taxon	**order**	**family**	**type**	**total ulnar length (mm)**	**Olecranon length (mm)**	**Index of fossorial ability (IFA)**
†*Xenocranium pileorivale*	†Palaeanodonta	†Epoicotheriidae	unknown	38.46	22.08	134.7
Amblysomus hottentotus	Afrosoricida	Chrysochloridae	subterranean	17.56	8.96	104.2
Priodontes maximus	Cingulata	Dasypodidae	fossorial	131.96	67.07	103.4
Cabassous centralis	Cingulata	Dasypodidae	fossorial	58.15	27.88	92.1
†*Pentapassalus pearcei*	†Palaeanodonta	†Epoicotheriidae	unknown	55	26	89.7
†*Naraboryctes philcreaseri*	**Notoryctemorphia**	**Notoryctidae**	**unknown**	17.9	8.4	88.4
Notoryctes typhlops	**Notoryctemorphia**	**Notoryctidae**	**subterranean**	16.1	7.5	87.2
Scaptochirus moschatus	Eulipotyphla	Talpidae	subterranean	15.93	7.36	85.9
Scapanus orarius	Eulipotyphla	Talpidae	subterranean	16.95	7.8	85.2
Euphractus sexcinctus	Cingulata	Dasypodidae	fossorial	70.83	30.72	76.6
Spalax giganteus	Rodentia	Spalacidae	subterranean	49.81	21.44	75.6
Chaetophractus villosus	Cingulata	Dasypodidae	fossorial	60.44	25.84	74.7
Dasypus novemcinctus	Cingulata	Dasypodidae	fossorial	76.63	32.58	74.0
Nannospalax leucodon	Rodentia	Spalacidae	subterranean	33.3	14.04	72.9
Talpa europaea	Eulipotyphla	Talpidae	subterranean	18.27	7.57	70.7
Scalopus aquaticus	Eulipotyphla	Talpidae	subterranean	17.97	7.44	70.6
Eremitalpa granti	Afrosoricida	Chrysochloridae	subterranean	12.16	4.98	69.4
†*Mesoscalops montanensis*	?Eulipotyphla	†Proscalopidae	unknown	24.83	9.6	63.0
Manis pentadactyla	Pholidota	Manidae	non-burrowing	60.7	23.46	63.0
Parascalops breweri	Eulipotyphla	Talpidae	subterranean	15.66	6.04	62.8
†*Palaeanodon ignavus*	†Palaeanodonta	†Metacheiromyidae	unknown	71	27	61.4
Tolypeutes matacus	Cingulata	Dasypodidae	non-burrowing	42.71	16.1	60.5

and *N. typhlops*, we calculated IFA based on our own measurements, whereas values for other taxa were calculated from measurements for total ulnar length and olecranon length given in Hopkins and Davis (2009).

Our phylogenetic analysis is based on the total evidence matrix used by Beck et al. (2014), specifically the version that includes character scores from isolated tarsals tentatively referred to *Yalkaparidon*. This matrix comprises 258 morphological characters and 9012 bp from five nuclear genes, namely *APOB* (exon 26), *BRCA1* (exon 11), *RBP3* (exon 1), *RAG1*, and *VWF* (exon 28), and includes a range of fossil and extant metatherians and non-metatherian outgroups (see Beck et al., 2014, and supplementary information for full details). We subdivided character 192 of Beck et al. (2014), such that presence/absence of the transverse canal foramen and its position (if present) are now treated as separate characters (characters 192–193), and hence the morphological matrix used here comprises a total of 259 characters. We also deleted the indels and retroposons included by Beck et al. (2014) because we used a total evidence dating approach (see below) and it is not obvious how rare genomic changes should be treated in this framework. We added *Naraboryctes* to this matrix, with character scores based on the craniodental and postcranial material described by Archer et al. (2011) and here. As in Beck et al. (2014), an appropriate partitioning scheme for the nuclear sequence data was determined using PartitionFinder (Lanfear et al., 2012), with initial partitioning by gene and codon position, and assuming linked branch lengths. Only models implemented by MrBayes were tested, using the "greedy" heuristic search algorithm, with the Bayesian Information Criterion used for model selection. The morphological partition was assigned the Mk model (Lewis, 2001), assuming that only parsimony-informative characters were scored, and with a gamma distribution to model rate heterogeneity between characters. As in Beck et al. (2014), multistate morphological characters representing putative morphoclines were ordered.

We employed a Bayesian total evidence dating approach (Ronquist et al., 2012a; Beck and Lee, 2014), which simultaneously estimates phylogeny and divergence times for both extant and fossil taxa, as implemented in MrBayes 3.2.2 (Ronquist et al., 2012b). Each terminal taxon was assigned an age: Recent taxa were assigned a point estimate of 0 Ma, whilst each fossil taxon was assigned an age range as a hard-bounded uniform prior, based on current age estimates (see supplementary information for full justification). The age of the root was also constrained as an offset exponential prior, with a minimum of 176.15 Ma and a mean (expectation) of 201.3 Ma. The minimum is based on the minimum radiometric age of the Queso Rellado locality of the Cañadon Asfalto Formation (Cúneo et al., 2013), which contains the oldest known putative crown-group mammals, *Asfaltomylos* and *Henosferus*, which are usually recovered as stem-monotremes in published phylogenetic analyses (e.g. Rougier et al., 2007; Bi et al., 2014). The mean corresponds to the Triassic-Jurassic boundary, and is broadly congruent with recent molecular estimates for the age of Mammalia (Meredith et al., 2011; dos Reis et al., 2012; 2014). Analysis of eutherian mammals suggests that total evidence dating in which only the age of the root is constrained can result in implausibly ancient divergence dates for at least some nodes (Beck and Lee, 2014); we therefore specified 13 additional topological and temporal constraints on internal nodes, with ages specified as offset exponential priors, namely: Theria, Marsupialia, Didelphidae, Didelphinae, crown-group Australidelphia, Dasyuridae, Dasyurinae, Peramelidae, Diprotodontia, Phalangerida, Petauroidea, Macropodidae and Vombatiformes (see supplementary information for full details). To assist convergence of the Bayesian analyses, monophyly of Eutheria and Metatheria was also enforced *a priori*, but the ages of these nodes were not calibrated.

The independent gamma rates (IGR) model was used (Ronquist et al., 2012a), with a single clock model applied to the entire nuclear sequence partition and a separate clock model applied to the morphological partition. The MrBayes analysis comprised four runs of four chains, each run for 15 million generations and with the temperature of the heated chains increased to 0.2. A burn-in fraction of 25% (i.e. 3.75 million generations) was specified; examination of plots of log likelihood against number of generations revealed that stationarity and convergence between chains had been achieved prior to this. The post-burnin trees were then summarised using majority-rule consensus, with all compatible partitions retained. Bayesian posterior probabilities (BPPs) were used as measures of clade support. The MrBayes file used in our analysis and the post-burnin majority-rule consensus that resulted are included in supplementary information.

To calculate the time of inactivation of *RBP3* in the notoryctemorphian lineage we used the general approach of Chou et al. (2002; see also Zhang et al., 2008). We first pruned our *RBP3* exon 1 alignment and the final consensus tree from our dated total evidence analysis so that only extant marsupials were retained (i.e. all fossil taxa and the monotreme outgroups *Ornithorhynchus* and *Tachyglossus* were deleted). We then deleted all codon positions in the pruned alignment that contained insertions. The modified *RBP3* alignment and pruned tree were then used to calculate the ratio of non-synonymous substitutions per non-synonymous site to synonymous substitutions per synonymous site (ω, also referred to as d_N/d_S, or K_a/K_s). Using the codeml package of PAML 4.7 (Yang, 2007), we firstly calculated ω for all branches, and then calculated ω separately for: 1) the branch leading to *Notoryctes* (the "foreground" branch; ω_f), and 2) all other branches (the "background" branches; ω_b). We used a likelihood ratio test to compare the relative fit of the two models (i.e. single ω, versus ω_f for *Notoryctes* and ω_b for all other branches), with critical values taken from a χ^2 distribution with a single degree of freedom (see Jansa and Voss, 2011). Values for ω_f and ω_b were then entered into the equation of Zhang et al. (2008: supplementary materials), to calculate the time of gene inactivation (T_N): $T_N = T((\omega_f - \omega_b)/(1- \omega_b))$, where T is the estimated time of divergence of the *Notoryctes* lineage (which was taken from the results of our total evidence dating analysis). This method assumes that, after a gene becomes inactive, ω for that gene becomes 1 (i.e., that non-synonymous substitutions and synonymous substitutions occur with the same frequency).

Anatomical description

General. Most of the limb bones of *Na. philcreaseri* discovered to date are missing the epiphyses, indicating that the epiphyseal sutures were unfused. Those that do preserve the epiphyses retain open sutures. In part, this may reflect the general marsupial pattern of most epiphyseal sutures remaining unfused throughout adult life (Geiger et al., 2014). However, based on their small size and very porous metaphyseal surfaces, at least some of the *Na. philcreaseri* specimens appear to represent juveniles (e.g., QM F57696, a right femur; QM F57703, a partial left ulna). By contrast, limb epiphyseal sutures are consistently fused in the skeletal specimens of *Notoryctes typhlops* and *N. caurinus* that we have examined, but these all appear to be adults based on the presence of a fully erupted permanent dentition (juvenile specimens of *Notoryctes* are exceptionally rare in scientific collections). Consistent closure of the epiphyseal sutures in the limbs of *Notoryctes* adults (which contrasts with the condition observed in most other marsupial species; Geiger et al. 2014) may reflect the high mechanical loadings their limbs are subjected to during digging; however, we note that Geiger et al. (2014) examined both fossorial and non-fossorial mammals and found no clear relationship between locomotor mode and the sequence of epiphyseal closure (see also Meier et al., 2013).

Scapula. Three partial scapulae are referable to *Na. philcreaseri* (see supplementary information), of which the most complete (QM F57716, which lacks only the acromion) is illustrated here (fig. 1a). In *Notoryctes* (and also some other burrowing mammals, such as talpids and chrysochlorids; Edwards, 1937; Reed, 1951; Puttick and Jarvis, 1977: fig. 3; Gasc et al., 1986), the scapular spine is oriented roughly parallel to the anterior thoracic vertebral column; hence the so-called "dorsal" (or "vertebral") border of the scapula is actually positioned caudally (rather than dorsomedially, towards the vertebral column), the "cranial" border is positioned dorsomedially, and the "caudal" (or "axillary") border is positioned ventrolaterally (Warburton, 2006). Based on its morphology, it seems likely that the scapula was similarly oriented in *Na. philcreaseri*. Nevertheless, to avoid confusion and to maintain consistency with anatomical descriptions of other mammals, we will refer to "cranial", "dorsal" and "caudal" borders in the scapula of *Na. philcreaseri* and *Notoryctes* following the terminology of, *inter alia*, Schaller (1992) and Evans (1993).

In dorsal view, the scapula appears narrow and elongate compared to those of most other marsupials. The supraspinous fossa is subtriangular in shape, and much larger in surface area than the infraspinous fossa. The infraspinous fossa is elongate and uniform in breadth along its length; its length-to-width ratio is approximately 10:1. Although slightly damaged in all three specimens, the scapular spine is clearly well-developed along its entire length, and its glenoid third is markedly broadened, slightly overhanging the infraspinous fossa. The angle between the "cranial" and "dorsal" borders of the scapula is approximately 80°, but is smoothly rounded. The "dorsal" border is short, rounded, and thickened for muscle attachment (principally the m. rhomboideus).

The glenoid third of the "caudal" border is markedly raised, forming a prominent secondary scapular spine that is separated from the scapular spine by the intervening infraspinous fossa. Although slightly damaged in QM F57716, the "caudal" angle appears rounded, thickened and slightly extended "caudally" (parallel to the "dorsal" border), for attachment of the m. teres major. The subscapular fossa is smoothly concave. The glenoid is large relative to the size of the supra- and infraspinous fossae, and the glenoid cavity is elliptical and relatively long. A small raised area from the "cranial" side of the glenoid cavity marks the coracoid process. The acromion is not preserved in any of the three specimens.

The elongate scapula of *Na. philcreaseri* bears a strong resemblance to that of *Notoryctes* (fig. 1b) and is broadly similar in size: maximum length of QM F57716 is 15.7 mm, compared to 13–13.5 mm in *N. caurinus* and 14.3–18.4 mm in *N. typhlops*. However, the modifications of the muscular attachment sites are markedly less extreme in the fossil species. Most notably, the "cranial" and "caudal" angles of the scapula (for attachment of the m. subscapularis and m. teres major respectively) appear to be gently rounded in *Na. philcreaseri* (although the caudal angle is slightly damaged in QM F57716, and hence its exact shape when intact is unclear), whereas in *Notoryctes* they are elongated and modified into recurved, hook-shaped processes, particularly the "caudal" angle, giving the bone an overall fan shape. *Notoryctes* also has a prominent postscapular fossa "caudal" to the secondary scapular spine,

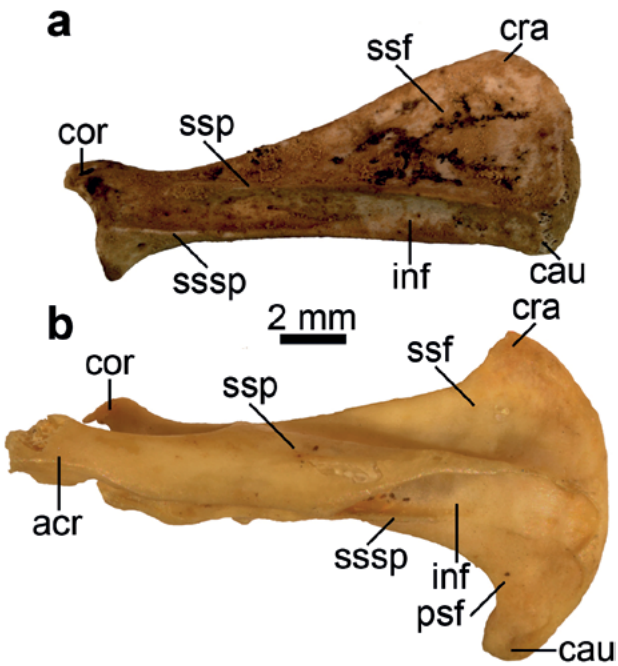

Figure 1. Comparison of scapulae of *Naraboryctes philcreaseri* and *Notoryctes typhlops* in lateral view: a, left scapula of *Naraboryctes philcreaseri* (QM F57716); b, right scapula (reversed) of *Notoryctes typhlops* (SAM M637). Abbreviations: acr, acromion process; cau, "caudal" angle; cor, coracoid process; cra, "cranial" angle; inf, infraspinous fossa; psf, postscapular fossa; ssf, supraspinous fossa; ssp, scapular spine; sssp, secondary scapular spine.

reflecting enlargement of the scapular (long) head of the m. triceps brachii. Enlargement of the triceps is common in fossorial mammals, particularly scratch diggers, and is also associated with elongation of the olecranon on the ulna (resulting in a larger IFA; Windle and Parsons, 1899; Taylor, 1978; Gasc et al., 1986; Stein, 1986; Lagaria and Youlatos, 2006; Warburton, 2006; Warburton et al., 2013). In *Na. philcreaseri*, the development of the secondary scapular spine reflects enlargement of the triceps compared to non-fossorial mammals. However, the absence of a postscapular fossa suggests that this muscle was probably not as well developed in *Na. philcreaseri* as it is in species of *Notoryctes*. The scapular spine is markedly broadened over two-thirds of its length in *Notoryctes*, towards the glenoid end, whereas only a third of the scapular spine is broadened in *Na. philcreaseri*. Furthermore, in *Notoryctes*, the scapular spine curves towards the secondary scapular spine, forming a tube-like structure that almost completely encloses the infraspinous fossa and infraspinatus muscle (this feature is better developed in *N. typhlops* than in *N. caurinus*; Warburton, 2006); no such tube is present in *Na. philcreaseri*.

Humerus. 31 humeri referable to *Na. philcreaseri* are known (see supplementary information). Their morphology is clearly indicative of fossoriality, and they are very similar in size and overall shape to those of *Notoryctes* species (see brief description by Archer et al., 2010: appendix 1). Most have lost their proximal and distal epiphyses. The specimen illustrated here, QM F57719, has the epiphyses in place, but the epiphyseal sutures remain unfused (figs. 2a, c).

The humeral head is large relative to the length of the bone, roughly hemispherical in shape, and protrudes posteromedially. The proximal tubercles are relatively low and broad; the greater tubercle extends slightly higher than the humeral head, while the lesser tubercle is slightly lower. The greater tubercle bears a short proximal crest, and is more than twice the breadth of the much smaller, ovoid lesser tubercle. The bicipital (intertubercular) groove is moderately broad and deep, and somewhat displaced medially due to the disproportionate sizes of the tubercles. The humeral neck is deeply constricted, particularly on its posterior aspect. The proximal half of the humeral shaft is relatively robust, and is marked by broad rugosities cranially and a broad sulcus caudally. The deltopectoral crest is massive and protrudes cranially and laterally from roughly the midpoint of the humeral shaft. This crest is thick and robust, with numerous rugosities, and its proximal end is distinctly concave in cranial view. Distal to this, a crest that appears continuous with the deltopectoral crest sweeps distally and medially, toward the medial epicondyle and over the supratrochlear foramen (which is proximal to the medial edge of the trochlea), giving the impression that the distal and proximal halves of the humerus are twisted relative to each other. Distally, the humerus broadens rapidly, primarily due to massive enlargement of the medial epicondyle; the maximum distal width of the humerus is slightly less than half its length. The medial epicondyle projects medially and is long and robust, with a bluntly rounded terminus. The trochlea and capitulum are smoothly contiguous, with only a slight medial constriction, and the combined articular surface is broad and convex. The coronoid

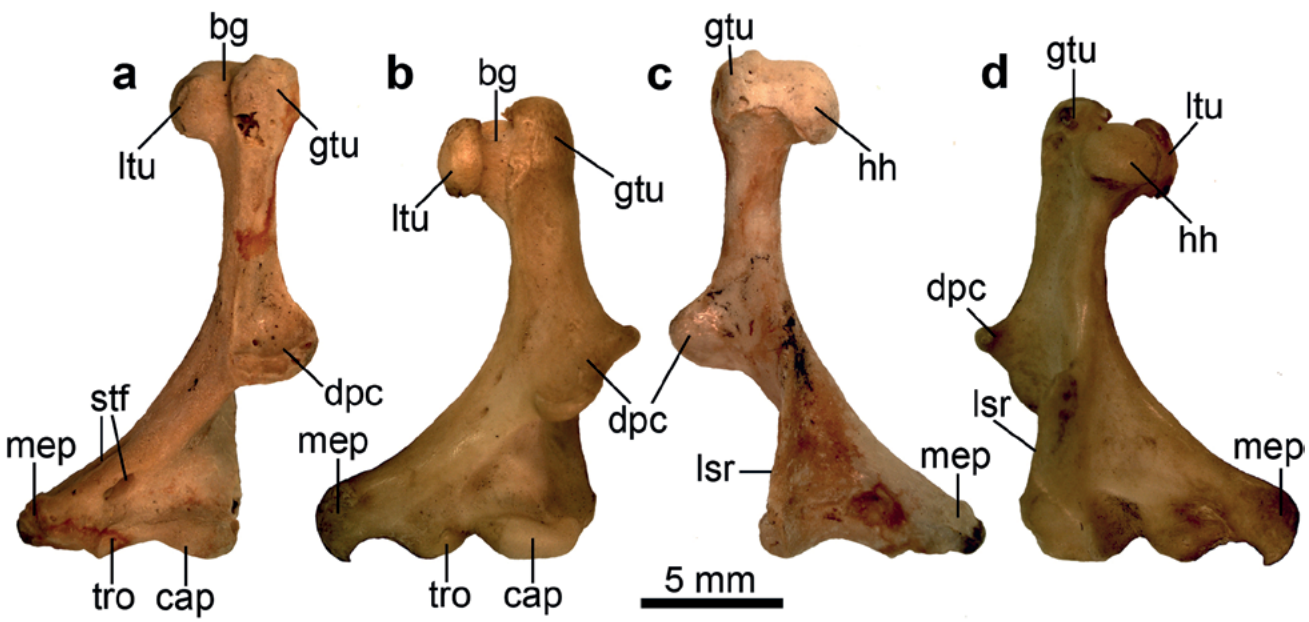

Figure 2. Comparison of humeri of *Naraboryctes philcreaseri* and *Notoryctes typhlops*: a, left humerus of *Naraboryctes philcreaseri* (QM F57719) in cranial view; b, right humerus (reversed) of *Notoryctes typhlops* (SAM M637) in cranial view; c, QM F57719 in caudal view; d, SAM M637 (reversed) in caudal view. Abbreviations: bg, bicipital groove; cap, capitulum; dpc, deltopectoral crest; gtu, greater tuberosity; hh, humeral head; lsr, lateral supracondylar ridge; ltu, lesser tuberosity; mep, medial epicondyle; stf, supratrochlear foramen; tro, trochlea.

fossa, proximal to the trochlea, is broad and shallow. The lateral epicondyle extends only slightly beyond the lateral border of the capitulum. The lateral supracondylar ridge is strongly developed, and extends proximally for more than one-third of the length of the humeral diaphysis, before merging with the mid-posterior surface of the shaft.

Although very robust compared to the humeri of non-fossorial mammals, the humerus of *Na. philcreaseri* is proportionately somewhat more elongate and gracile than that of *Notoryctes* (figs. 2b, d): maximum length and distal width of the most complete adult humeri of *Na. philcreaseri* (QM F23710, F57652 and F57719) are 15.1-17.2 mm and 7.9-8.3 mm respectively, whereas in *N. caurinus* they are 11.9-12.7 mm and 7.5-8.2 mm, and in *N. typhlops* they are 13.4-15.6 mm and 7.6-10.4 mm. As noted by Archer et al. (2011: appendix 1), the humeral shaft is oval in cross-section in *Na. philcreaseri*, rather than triangular as it is in *Notoryctes*, the proximal surface of the deltopectoral crest is concave rather than convex, and a supratrochlear foramen is present whereas this foramen is absent in *Notoryctes*. In addition, the bicipital groove is distinctly shallower than it is in *Notoryctes*, and the deltopectoral crest, medial epicondyle and lateral supracondylar ridge are all smaller and less strongly developed in the fossil species. A further key difference is that in *Notoryctes* the capitulum is relatively broader and more cylindrical, and there is a distinct separation of the capitulum and trochlea, whereas these form a single, continuous articular surface in *Na. philcreaseri*.

Radius. The 11 radii attributed here to *Na. philcreaseri* (see supplementary information) are very robust for their overall size. Both the proximal and distal ends of the bone are expanded, and are approximately equal width, although most are missing the proximal and distal epiphyses; QM F57679, however, is complete and is illustrated here (figs. 3a, c). The fovea is ovoid and smoothly concave, and demarcated by a well-marked border. Along the posterolateral aspect of the shaft is an obvious groove; this groove is also present in *Notoryctes*, where it houses a tendinous sheet (the interosseous membrane) that binds the shafts of the radius and ulna together (Warburton, 2006). The distal end of the radius (for the radiocarpal articulation) is very broad, and possesses a short styloid process. In its general size, shape and robustness, the radius of *Na. philcreaseri* is very similar to that of *Notoryctes* (figs. 3b, d), although this bone is slightly longer in the fossil species (10.7 mm in QM F57679; 10.3 mm in QM F57680) than in either *N. caurinus* (6.9-7.2 mm) or *N. typhlops* (7.4-9.3 mm).

Ulna. 30 ulnae referable to *Na. philcreaseri* are known (see supplementary information). Together with the humerus, the ulna of *Na. philcreaseri* arguably exhibits the most obvious evidence of fossorial adaptations, as briefly discussed by Archer et al. (2011: appendix 1). The ulnar shaft is robust and relatively deep in the cranial-caudal plane, but narrow mediodistally. The olecranon is long, robust and somewhat curved medially; measured from the distal margin of the trochlear notch (following Hopkins and Davis, 2009), it forms more than 40% of the total length of the ulna, although the exact percentage is uncertain as none of the ulnae of *Na. philcreaseri* are fully intact; most are missing either the proximal or distal epiphysis or both. The most complete specimen, QM F57706, is illustrated here (figs. 4a, c e) and was used to calculate IFA for *Na. philcreaseri* (table 1); however, QM F57706 lacks the distal epiphysis, and hence the calculated IFA is undoubtedly a slight overestimate (see below).

The trochlear (semilunar) notch is moderately deep, and its distal (coronoid) surface is very steep in comparison to the proximal (anconeal) surface. The trochlear notch is broad and lies in somewhat oblique alignment, from proximomedial to distolateral. The proximal anconeal process is long and extends laterally. A crest extends proximally from the medial margin of the proximal anconeal process, along the cranial aspect of the olecranon. A crest also extends distally along the cranial aspect of the ulnar shaft. The broad radial notch is on the lateral side of the anconeal process, slightly distal to the articular surface for the trochlea of the humerus. Medial and lateral coronoid processes surround the radial notch in a slightly oblique orientation. In medial view, a very prominent flexor sulcus extends from the proximal ulnar shaft onto the olecranon.

The ulna of *Na. philcreaseri* resembles that of *Notoryctes* (figs. 4b, d, f), and is similar in size; total preserved length of QM F57706 is 17.9 mm (when intact, this bone may have been 0.5-1.0 mm longer), whereas the length of this bone is 13.4-14.2 mm in *N. caurinus* and 15.4-18.7 mm in *N. typhlops*. However, the ulnar shaft is proportionately longer and mediolaterally narrower in *Na. philcreaseri*, and therefore appears more gracile. The morphology of the ulnar articular surfaces are very similar between the fossil and extant species, particularly in the distinct distal displacement of the radial articulation; however, the trochlear notch is not as broad and

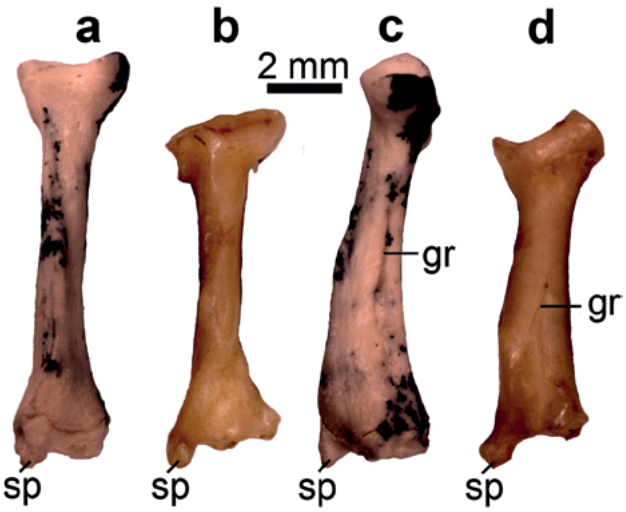

Figure 3. Comparison of radii of *Naraboryctes philcreaseri* and *Notoryctes typhlops*: a, left radius of *Naraboryctes philcreaseri* (QM F57679) in cranial view; b, right radius (reversed) of *Notoryctes typhlops* (SAM M637) in cranial view; c, QM F57679 in lateral view; d, SAM M637 (reversed) in lateral view. Abbreviations: gr, groove for interosseous membrane (tendinous sheet binding shafts of radius and ulna together); sp, styloid process.

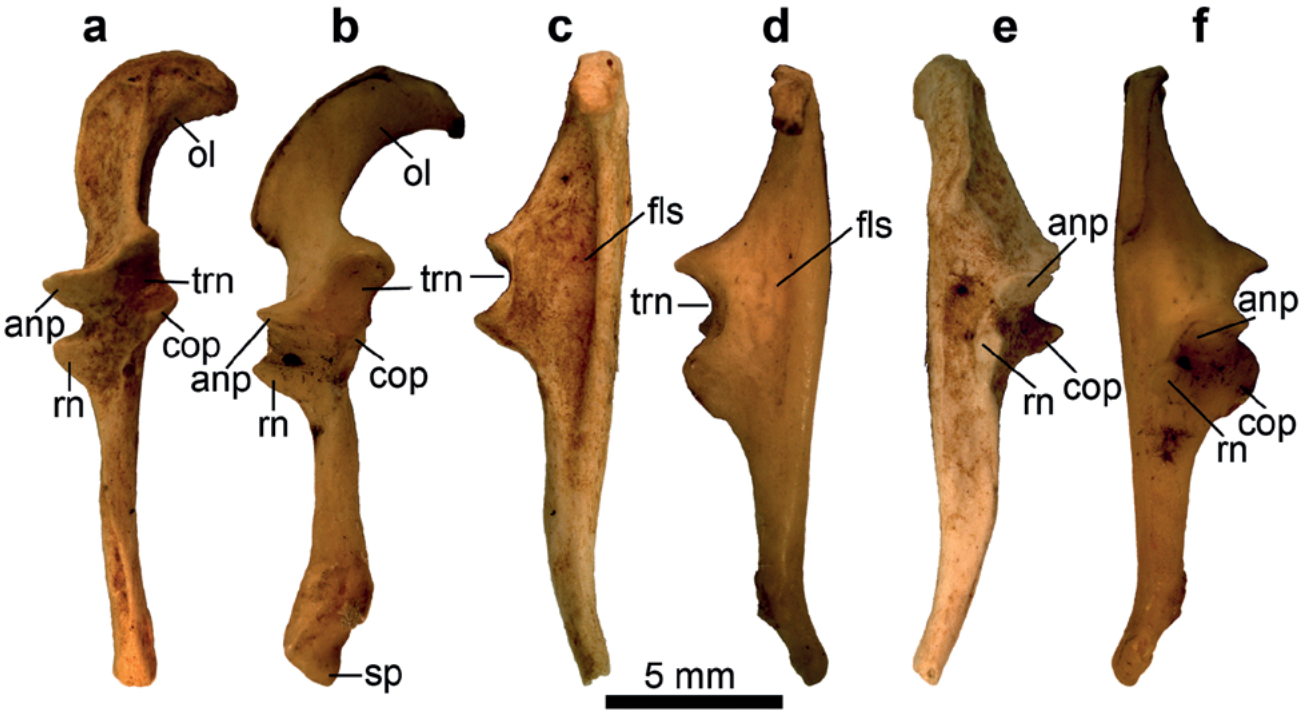

Figure 4. Comparison of ulnae of *Naraboryctes philcreaseri* and *Notoryctes typhlops*: a, right ulna of *Naraboryctes philcreaseri* (QM F57706) in cranial view; b, right ulna of *Notoryctes typhlops* (SAM M637) in cranial view; c, QM F57706 in medial view; d, SAM M637 in medial view; e, QMF 57706 in lateral view; f, SAM M637 in lateral view. Abbreviations: anp, anconeal process; cop, coronoid process; fls, flexor sulcus; ol, olecranon; rn, radial notch; sp, styloid process; trn, trochlear notch.

the radial notch not as deep in *Na. philcreaseri*. Interestingly, in QM F57706 at least, the flexor sulcus on the medial aspect of the ulna is deeper in *Na. philcreaseri* than in *Notoryctes*. The olecranon is also less curved medially in the fossil species; as a result, although the total length of the olecranon, measured following its curvature, is clearly proportionately greater in *Notoryctes*, the anteroposterior length of the olecranon, measured parallel to the ulnar shaft, is proportionately similar between the fossil and extant species.

Femur. The 17 femora referred here to *Na. philcreaseri* (see supplementary information) are highly distinctive (figs. 5a, c), but are broadly similar in size to femora of *Notoryctes* species; based on the three most complete *Na. philcreaseri* specimens (QM F57678, F57718, F57708), total length is 13.6-17.3 mm, compared to 12.4-14.1 mm in *N. caurinus* and 14.3-16.8 mm in *N. typhlops*. The femoral head is essentially spherical in shape. The greater trochanter is broad and laterally extended. In specimens in which the proximal femoral epiphyses are intact (e.g. QM F57678), the greater trochanter is very slightly lower than the femoral head. The lesser trochanter is broad and rounded in outline and does not extend proximally as far as the femoral head. In some specimens (e.g. QM F57708), the lesser trochanter is deeply excavated such that its cranial face forms a distinct 'pocket', whereas in others (e.g. QM F57678) a somewhat shallower, less well-defined depression is present. In caudal view, a small, shallow trochanteric fossa is visible in a quite lateral position, on the caudal face of the greater trochanter. The femoral shaft is robust for its length and oval in cross-section. The distal shaft flares towards the enlarged condylar region. The intercondylar groove is relatively broad. A large, anteroposteriorly-compressed process, the third trochanter, protrudes laterally from the mid-shaft. At the level of the third trochanter, the maximum transverse width of the femur is more than one-fifth of femoral length.

The femur of *Na. philcreaseri* is substantially modified from those of more generalised marsupials in its being particularly robust, the strong development (relative to absolute size) of the greater and lesser trochanters, and the presence of a very large third trochanter. In comparison to *Notoryctes* (figs. 5b, d), the femoral shaft of *Na. philcreaseri* is not as robust with respect to femoral length, nor is the greater trochanter as robust or broad. The lesser trochanter is located in a more proximocaudal position in *Notoryctes*, such that it is proximodistally level with the femoral head (Warburton, 2006: fig. 13). *Na philcreaseri* retains a small trochanteric fossa, whereas no such fossa is found in *Notoryctes*. A particularly striking difference between *Na. philcreaseri* and *Notoryctes* is that the latter lacks a distinct third trochanter. However, the greater trochanter of *Notoryctes* is very large and extends distally as a wing-like process along

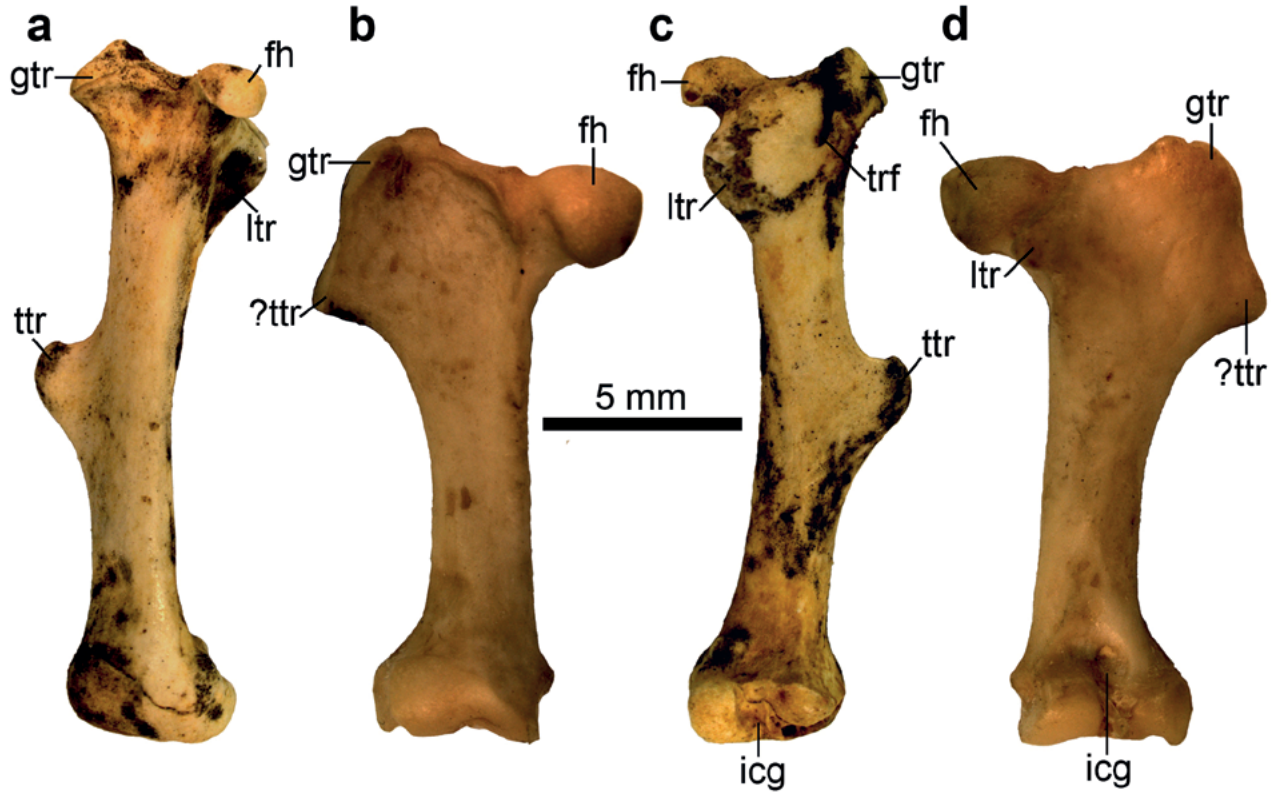

Figure 5. Comparison of femora of *Naraboryctes philcreaseri* and *Notoryctes typhlops*: a, right femur of *Naraboryctes philcreaseri* (QM F57678) in cranial view; b, right femur of *Notoryctes typhlops* (SAM M637) in cranial view; c, QM F57678 in caudal view; d, SAM M637 in caudal view. Abbreviations: fh, femoral head; gtr, greater trochanter; icg, intercondylar groove; ltr, lesser trochanter; trf, trochanteric fossa; ttr, third trochanter.

the lateral margin of the proximal quarter of the femur; we suspect that this process originated via ancestral fusion of the greater and third trochanters, with the distal end of this process homologous with the third trochanter of *Na. philcreaseri*, as we discuss in more detail below (see Discussion).

Tibia. The five tibiae described here are referred to *Na. philcreaseri* (see supplementary information) on the basis of their size and unusual morphology (figs. 6a, c), which somewhat resembles that observed in *Notoryctes* (figs. 6b, d). All known specimens are missing the proximal and distal epiphyses, with preserved lengths ranging from 10.2 to 12.7 mm. By comparison, intact tibial length is 10.1-10.5 mm in *N. caurinus* and 12.6-13.6 mm in *N. typhlops*. The most distinctive feature of the *Na. philcreaseri* tibiae is the massively developed tibial crest on the cranial aspect, which extends along the proximal two-thirds of the length of the tibia and more than doubles its craniocaudal depth. The development of the massive tibial crest is strongly reminiscent of the strong development of the same feature in *Notoryctes*. Unlike the flat, blade-like tibial crest of *Notoryctes*, however, the crest in *Na. philcreaseri* is curved in cross-section, such that it is slightly convex on its medial surface and slightly concave on its lateral surface. In addition, whereas the crest is most extensive cranially at its proximal end (adjacent to the articulation with the femur) in *Notoryctes*, in *Na. philcreaseri* it is most extensive more distally, reaching its maximum extent about two-thirds along its length from the proximal end of the tibia. The tibial crest of *Notoryctes* is mediolaterally broad and concave at its proximal end, for articulation with the distinctive enlarged patella. By contrast, the crest in *Na. philcreaseri* is mediolaterally narrow, and there is no sulcus that might have housed a patella. It is therefore unclear whether or not a patella was present in *Na. philcreaseri*. Absence of the proximal and distal epiphyses also means that the precise morphology of the femoral and tarsal articular surfaces is unknown; in particular, it is unclear whether or not the peculiar, rounded process present posterolaterally at the proximal end of the tibia in *Notoryctes* (which articulates with the lateral condyle of the femur and also with the fibula; Stirling, 1891: 179) was present in *Na. philcreaseri*. However, proximally, it appears that the medial condyle was probably slightly larger than the lateral condyle in *Na. philcreaseri*, as in *Notoryctes*. The distal shaft is also short and very robust, although slightly less so than in *Notoryctes*.

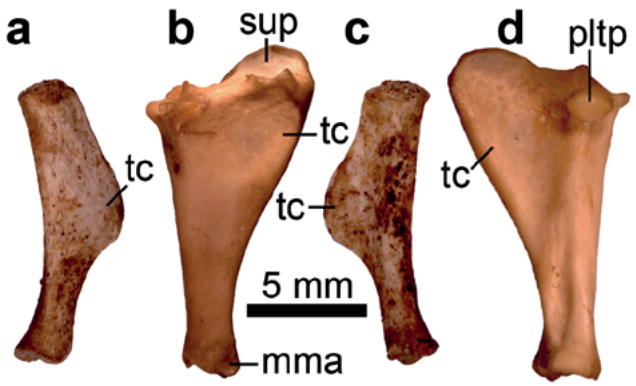

Figure 6. Comparison of tibiae of *Naraboryctes philcreaseri* and *Notoryctes typhlops*: a, left femur of *Naraboryctes philcreaseri* (QM F57686) in medial view; b, left femur of *Notoryctes typhlops* (SAM M637) in medial view; c, QM F57686 in lateral view; d, SAM M637 in lateral view. Abbreviations: mma, medial malleolus; pltp, posterolateral tibial process for articulation with lateral femoral condyle and fibula; sup, sulcus for patella; tc, tibial crest.

Functional interpretation of the postcranial skeleton of *Naraboryctes philcreaseri*

Forelimb. The scapula of *Na. philcreaseri* (fig. 1a) is elongate and narrow in comparison to those of more generalised mammals. In *Notoryctes* (fig. 1b) and many other fossorial and subterranean mammals, the scapula is similarly elongate and narrow (Reed, 1951; Gasc et al., 1986; Warburton, 2006; Salton and Sargis, 2008). In these forms, this morphology reflects the reduction of dorsally-placed muscles between the thoracic vertebral column and scapula (e.g. the m. rhomboideus), which allows posterior rotation of the scapula. It is also correlated with the more cranio-caudal alignment of the long axis of the scapula (Reed, 1951; Puttick and Jarvis, 1977; Gasc et al., 1986; Warburton, 2006), which results in enhanced mobility of the pectoral girdle along the cranial-caudal axis (as demonstrated in *Eremitalpa*; Gasc et al., 1986). As a result, the pectoral girdle is highly mobile, facilitating protraction and retraction of an extended forelimb, as is required for scratch-digging (Hildebrand, 1985; Nevo, 1999: 71).

The humerus (figs. 2a, c), radius (figs. 3a, c) and ulna (figs. 4a, c, e) of *Na. philcreaseri* are all very robust for their length, and the articular surfaces of these bones are relatively large in surface area. Short, robust limb bones are characteristic of semi-fossorial and fossorial mammals (Casinos et al., 1993; Farina and Vizcaino, 1997; Vizcaino et al., 1999; Campione and Evans, 2012), being better able to withstand the high muscular and reaction forces acting through the bones during digging (Hildebrand and Goslow, 2001; Elissamburu and Vizcaíno, 2004). The relatively large surface area of humeral head, capitulum and radial fovea of *Na. philcreaseri* would have acted to improve the stability and structure of the joint by spreading large mechanical forces over a greater area. Similarly enlarged articular surfaces are found in the forelimb of many other fossorially-adapted mammals, including chrysochlorids (Gasc et al., 1986) and anteaters (Taylor, 1978).

The enlarged and strengthened muscle attachment sites of the forelimb of *Na. philcreaseri*, notably the development of a secondary spine on the scapula (fig. 1a), the enlarged deltopectoral crest and medial epicondyle of the humerus (figs. 2a, c), and the proportionately robust and elongate olecranon of the ulna (fig. 4a), are also all characteristic of a fossorial or subterranean lifestyle (Reed, 1951; Lehmann, 1963; Taylor, 1978; Thorington et al., 1997; Warburton, 2006; Warburton et al., 2013). Collectively, they reflect enlargement of the m. triceps longus, mm. pectorales, m. flexor carpi radialis, and m. flexor carpi ulnaris and m. flexor digiti profundus, each of which contribute during the power stroke of digging and thus require increased power in order to act against the resistance of the substrate.

Besides muscle enlargement, power can also be increased by migration of muscle attachment sites to improve mechanical advantage: typically, fossorial mammals enhance mechanical advantage by increasing the length of the in-lever relative to the out-lever length (Lehmann, 1963; Nevo, 1979; Nevo, 1999; Hildebrand and Goslow, 2001). The distally placed deltopectoral crest of the humerus (figs. 2a, c) and greatly enlarged olecranon of the ulna (fig. 4a) of *Na. philcreaseri* would have acted to functionally increase the in-lever length of their respective muscles by moving the insertions further from the joint across which they act, while the relatively short limb bones would have reduced the length of the out-lever. In comparison to other fossorial mammals, the deltopectoral insertion is more distally placed in *Na. philcreaseri* than in digging armadillos (MacAlister, 1875a; Macalister, 1875b; Burne, 1901; Hildebrand and Goslow, 2001) and fossorial rodents (Lehmann, 1963), but less distally placed than the homologous structure in some chrysochlorids (Gasc et al., 1986). Similarly, the elongate medial epicondyle of *Na. philcreaseri* (figs. 2a, c) reflects improved mechanical advantage by providing a long lever arm of the forearm flexor musculature (as well an enlarged area for muscle attachment), for strong flexion of the wrist against the substrate during digging. This is convergent with other scratch diggers, particularly where the elbow is somewhat extended during limb retraction in the power-stroke of digging (Gasc et al., 1986; Warburton, 2006). It is also characteristic of fossorial mammals that utilise a partially abducted (half-sprawling) or sprawling posture of the carpus during digging (Gambaryan and Kielan-Jaworowska, 1997).

Turning now to the ulna, IFA for *Na. philcreaseri* is 88.4, which is slightly higher than that for *Notoryctes typhlops* (87.2; see table 1). However, the specimen used to calculate IFA in *Na. philcreaseri*, QM F57706, is missing the distal epiphysis (see fig. 4a, c, e) and so this value is undoubtedly a slight overestimate; the true value for *Na. philcreaseri* is probably the same as, or slightly less than, that for *N. typhlops*. It should also be noted that IFA is based on the anteroposterior length of the olecranon; it does not take into account the degree of medial curvature of the olecranon, which is greater in *Notoryctes* species (fig. 4b; Warburton, 2006: fig. 9) than in *Na. philcreaseri* (fig. 4a). The IFA values for *Na philcreaseri* and *N. typhlops* are some of the highest seen in mammals

(table 1); of the taxa measured by Hopkins and Davis (2009), only the chrysochlorid *Amblysomus hottentotus* (which is subterranean), the dasypodids *Priodontes maximus* and *Cabassous centralis* (which are both fossorial), and the fossil epoicotheriid palaeanodonts *Xenocranium pileorivale* and *Pentapassalus pearcei* exhibit higher values. Other subterranean mammals, such as talpids and spalacid rodents are characterised by lower IFA values (table 1).

Hind limb. The femur of *Na. philcreaseri* is robust, and the greater and lesser trochanters are very large for a bone belonging to a mammal of this size (figs. 5a, c). The lateral expansion of the proximal femur compared to more generalised marsupials seen in *Na. philcreaseri* is largely due to enlargement of the greater trochanter. Lateral extension of the proximal femur is even more extreme in *Notoryctes*, due to its very wide greater trochanter (figs. 5b, d). Although not as large as in *Notoryctes*, the transversely wide greater trochanter of *Na. philcreaseri* would have improved the mechanical advantage of the gluteal muscles for limb abduction by increasing the length of the in-lever; this suggests a strongly abducted posture of the hind limbs, most likely to brace the hind part of the body during digging, but potentially also during the propulsive phase of locomotion.

The prominent third trochanter protruding laterally from the midshaft of the femur of *Na. philcreaseri* is highly distinctive (figs. 5a, c). A much smaller, more proximally-positioned third trochanter occurs in caenolestids, vombatids and some stem-metatherians (Szalay and Sargis, 2001; Horovitz et al., 2008; Abello and Candela, 2010). However, no such distinct process is observed in *Notoryctes* (figs. 5b, d) or most other marsupials. Among placental mammals at least, the third trochanter (where present) is for attachment of the gluteal muscles. The gluteal musculature of *Notoryctes* is modified compared with that of other marsupials, due to the highly modified morphology of the pelvis and the expanded greater trochanter (Warburton, 2006). While there is no indication in the living species of an insertion by the gluteal musculature on the mid-lateral femur, the morphology of the femur of *Naraboryctes* may represent an adaptation for increasing the leverage of the gluteal muscles for limb abduction. If so, this may indicate that the hindlimbs were strongly abducted in *Na. philcreaseri* (at least during burrowing), which would be a plausible intermediate stage between the parasagittal stance of generalised terrestrial mammals and the highly specialised stance of *Notoryctes*, where the legs appear to project laterally from the body and no longer play a role in supporting the body off the substrate. In addition, among extant and fossil xenarthrans, a prominent third trochanter has been proposed as a mechanism to mitigate, by muscular action, bending forces acting through the femur (Milne and O'Higgins, 2012). The hypothesised shift to a strongly abducted hind limb position in *Na. philcreaseri*, potentially for bracing or active excavation of substrate, would tend to increase bending moments through the femur; if so, this may have favoured the evolution of enlarged gluteal musculature to mitigate these forces, with concomitant development of a large third trochanter. In *Notoryctes*, there is a well-developed crest extending from the greater trochanter along the proximal third of the length of the bone (figs. 5b, d). We suggest that this proximally-extended lateral crest in *Notoryctes* is the result of ancestral fusion of the third trochanter seen in *Na. philcreaseri* with the greater trochanter, and that the distal end of this crest in *Notoryctes* is homologous with the third trochanter of *Na. philcreaseri*.

Discriminant analysis

Compared to Hopkins and Davis' (2009) original "limbs only" dataset, our quadratic discriminant analysis based on a slightly expanded and modified dataset showed slightly better accuracy for discriminating burrowing from non-burrowing mammals (13.2% misidentified, versus 13.9% in Hopkins and Davis, 2009), but was somewhat less accurate at determining the degree of fossoriality, i.e. distinguishing between non-burrowing, fossorial and subterranean mammals (18.2% misidentified, versus 14.8% in Hopkins and Davis, 2009). In the "burrowing" versus "non-burrowing" analysis, *Na. philcreaseri* was identified as burrowing with very high probability (p = 0.99), and in the "non-burrowing" versus "fossorial" versus "subterranean" analysis it was identified as subterranean, again with very high probability (p =1.00). A plot of the first two canonical axes from the non-burrowing versus fossorial versus subterranean analysis indicates that the first axis encompasses 91.2% of the total variability, with subterranean taxa exhibiting the lowest values and non-burrowing taxa the highest values (fig. 7). *Na. philcreaseri* exhibits a very low value for the first canonical axis, even lower than for *N. typhlops*, and plots closest to the subterranean chrysochlorid *Eremitalpa granti* (fig. 7).

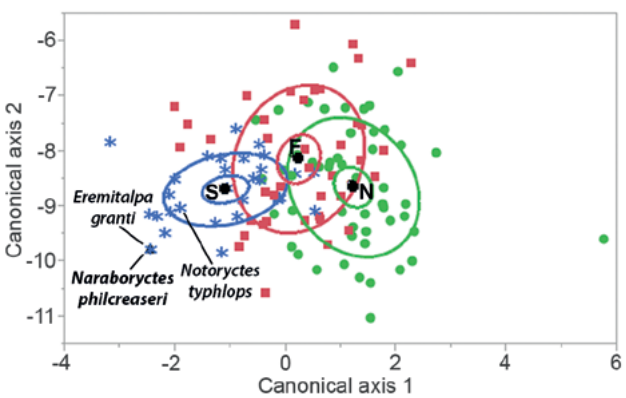

Figure 7. Plot of first two canonical axes from quadratic discriminant analysis of degree of fossoriality (non-burrowing versus fossorial versus subterranean) in mammals based on an expanded version of the "limbs only" dataset of Hopkins and Davis (2009). Non-burrowing species are represented by green circles, fossorial species by pink squares and subterranean species by blue asterisks. Inner ellipses represent 95% confidence intervals for the means for each class, whilst the outer ellipses represent the 50% prediction intervals. *Naraboryctes philcreaseri* is represented by a black triangle and was treated as unknown, but falls among subterranean species and is predicted to be subterranean with very high probability (p = 1.0). Abbreviations: F, fossorial; N, non-burrowing; S, subterranean.

Phylogeny and divergence times

The dated phylogeny that results from Bayesian analysis of our total matrix using the IGR clock model is given in Figure 8. The topology is broadly congruent with that found in analyses of a similar version of the matrix by Beck et al. (2014). As expected, *Na. philcreaseri* is recovered as sister-taxon to *Notoryctes*, with strong support (BPP = 0.91). Notoryctemorphia (i.e. *Naraboryctes* + *Notoryctes*) is sister to Peramelemorphia (i.e. *Echymipera* + *Perameles*), with Dasyuromorphia (i.e. *Dasyuroides* + *Dasyurus* + *Phascogale*) outside this, but support values for these two nodes are very low (BPP <0.5). There is somewhat stronger support (BPP = 0.71) for the clade comprising Notoryctemorphia, Peramelemorphia, Dasyuromorphia and *Yalkaparidon*, which corresponds to Agreodontia *sensu* Beck et al. (2014).

In terms of divergence times, the base of Agreodontia is estimated to be 55.2 MYA (95% HPD = 48.0-63.9 MYA), with Dasyuromorphia diverging at 54.4 MYA (95% HPD = 46.8-63.9 MYA), and the Notoryctemorphia-Peramelemorphia split estimated at 52.2 MYA (95% HPD = 43.6-60.7 MYA). The point estimate for the split between *Notoryctes* and *Naraboryctes* is 30.3 MYA, which is considerably older than the age of *Naraboryctes* inferred here (19.4 Ma old; 95% HPD = 16.0-22.6 Ma old). However, the 95% HPD for this split is wide (17.7-46.3 MYA) and overlaps the inferred age of *Na. philcreaseri*. Furthermore, the 95% HPD for the effective branch length leading to *Naraboryctes* (i.e. the estimated change relative to that inferred for the last common ancestor of *Naraboryctes* and *Notoryctes*) is 0.0000-0.0733 substitutions/site (= changes/character) for the morphological partition (see supplementary information); this encompasses the possibility that *Na.philcreaseri* exhibits no morphological apomorphies relative to the *Naraboryctes-Notoryctes* common ancestor. Thus, when 95% HPDs are taken into account, the age and morphology of *Na. philcreaseri* are both compatible with its being ancestral to *Notoryctes* (M.S.Y. Lee, pers. comm.).

RBP3 inactivation

Specifying separate values of ω for the *RBP3* alignment for *Notoryctes* (the "foreground" branch, ω_f) and for all other branches (the "background" branches, ω_b) did not result in a significantly better fit than the null model of a single value of ω for all branches ($p >> 0.05$). However, entering the values for ω_f (0.244) and ω_b (0.15635) into the equation of Zhang et al. (2008), and assuming that *Notoryctes* diverged from (*Echymipera* + *Perameles*) at 52.2 MYA (see above) gives an estimate of 5.4 MYA for the timing of inactivation of *RBP3* in the *Notoryctes* lineage, with a range of 4.5–6.3 MYA if the

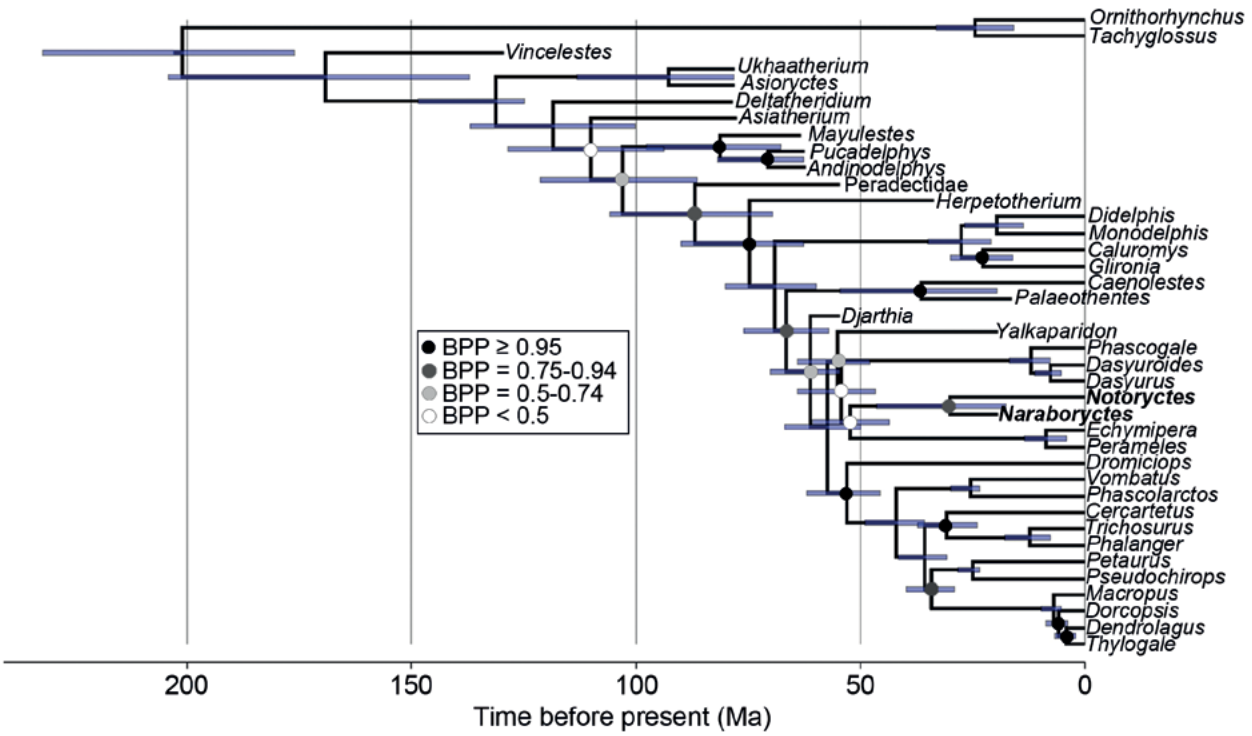

Figure 8. Dated total evidence phylogeny based on 259 morphological characters and 9012 bp of sequence data from five nuclear genes (*APOB*, *BRCA1*, *RBP3*, *RAG1*, and *VWF*) analysed using MrBayes 3.2.2 assuming the Independent Gamma Rates (IGR) clock model, with topological and temporal constraints applied to selected internal nodes (see supplementary information). *Notoryctes* and *Naraboryctes* are indicated in bold. Blue bars represent 95% highest posterior density intervals (HPDs) on the divergence times. Nodes without Bayesian posterior probability (BPP) were constrained *a priori*.

95% HPD for the time of divergence is taken into account (fig. 9; see above). This corresponds to the latest Miocene-earliest Pliocene, and considerably postdates the age of *Na. philcreaseri* (fig. 9), suggesting that *RBP3* was functional in this fossil taxon. Interestingly, it is similar to Mitchell et al.'s (2014) relaxed molecular clock estimate of 4.5 MYA for the divergence between the living species *Notoryctes typhlops* and *N. caurinus.*

Discussion

Qualitative functional analysis of the postcranial anatomy of *Na. philcreaseri* indicates that it was well-adapted for scratch-digging. Of particular significance are the narrow, elongate scapula with secondary scapular spine, very robust humerus with enormously enlarged deltopectoral crest and medial epicondyle, and greatly enlarged and medially-inflected olecranon of the ulna. All of these are characteristic of extant scratch-diggers, and of fossil mammals that have been interpreted to exhibit similar burrowing behaviour, such as the early Miocene meridiolestidan *Necrolestes* and the late Eocene epocoitheriid palaeanodonts *Epoicotherium* and *Xenocranium* (Turnbull and Reed, 1967; Rose and Emry, 1983). This interpretation is bolstered by the results of our quadratic discriminant analysis, in which *Na. philcreaseri* is predicted

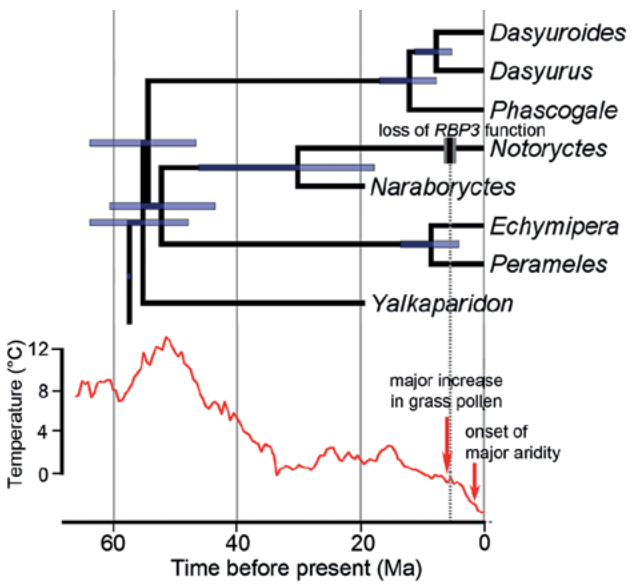

Figure 9. Part of the dated total evidence phylogeny shown in Figure 8, restricted to the clade Agreodontia (which includes Notoryctemorphia), with divergence dates compared to global temperatures and environmental change in Australia. The estimated time of inactivation of the *RBP3* gene in the *Notoryctes* lineage is indicated: the black bar represents the point estimate (5.4 MYA), whilst the grey bars represent 95% HPDs (4.5-6.3 MYA). The global temperature curve is modified from Zachos et al. (2001). The date for the major increase in grass pollen is taken from Martin and McMinn (1994: fig. 2) whilst the date for the onset of major aridity in Australia (~1.4-1.5 MYA) is taken from McLaren and Wallace (2010).

to be subterranean based on its limb proportions, and lies closest to the subterranean chrysochlorid *Eremitalpa granti* in our plot of the first two canonical axes. In addition, although the IFA value calculated for *Na. philcreaseri* (88.4) is undoubtedly a slight overestimate, it is almost identical to that for *N. typhlops* (87.2), and is greater than that for many fully subterranean mammals (table 1). In summary, all available morphological evidence supports the conclusion that *Na. philcreaseri* was a specialised, most probably subterranean, scratch-digger.

These results indicate that specialised fossorial, probably subterranean, behaviour originated in the notoryctemorphian lineage some time before the early Miocene. The Faunal Zone B deposits at Riversleigh from which all known specimens of *Na. philcreaseri* have been recovered appear to represent rainforest environments (Travouillon et al., 2009; Archer et al., 2011; Bates et al., 2014), and forests likely predominated throughout Australia until the middle-late Miocene (Martin, 2006). This may be an indication that the burrowing specialisations of fossil notoryctemorphians were well-suited to, and potentially evolved in, such closed forest environments. If so, the golden moles *Chrysospalax trevelyani* and *Huetia leucorhina* (which forage in or above leaf litter as well as digging burrows in the rainforests of sub-Saharan Africa; Bronner, 2013) and possibly other fossorially-adapted mammals that live in rainforest environments (e.g. the tenrec *Oryzorictes hova* of Madagascar, and the peramelemorphian *Microperoryctes murina* of New Guinea) may represent reasonable living analogues for early notoryctemorphians. However, rainforest soils are typically thin and do not appear favourable for the evolution of a truly subterranean lifestyle. Furthermore, Riversleigh appears to have been a karst environment during the early Miocene (Arena, 2004; Arena et al., 2014), and karst (including karst in rainforest) typically has exposed rocky surfaces only partially covered by thin soils (although deep, dirt-filled fissures may be present; D.A. Arena, pers. comm.). We therefore propose two further scenarios for the origin of specialised fossorial behaviour in notoryctemorphians.

It is interesting that all specimens of *Na. philcreaseri* collected to date are from sites at Riversleigh that are interpreted as representing cave deposits (Arena, 2004; Arena et al., 2014). An alternative hypothesis is therefore that notoryctemorphians acquired fossorial behaviours foraging for invertebrates within cave environments, burrowing through guano-rich cave floors. However, we note that no modern mammal or other terrestrial vertebrate of which we are aware occupies such a niche, nor is their compelling evidence for occupation of this niche by any other fossil vertebrate species. Furthermore, all Riversleigh sites representing the early Miocene Faunal Zone B appear to be cave deposits (D. A. Arena, pers. comm.). Thus, the presence of *Na. philcreaseri* fossils at these sites may simply be because notoryctemorphians only occurred in the Riversleigh area during the early Miocene, and are present in cave deposits because those are the only deposits preserved from this time period, not because they were cave-dwelling. Several other Riversleigh mammal species are known only from Riversleigh Faunal Zone B (and

hence are found only in cave deposits), including the thylacinids *Wabulacinus ridei* and *Ngamalacinus timmulvaneyi* (see Muirhead, 1997) and species of the miralinid possum *Durudawiri* (e.g. Crosby and Archer, 2000; Crosby, 2002), none of which are likely to have been cave-dwellers. However, remains of these species are admittedly much rarer than those of *Na. philcreaseri*. On the other hand, Rzebik-Kowalska (2013) reported very large numbers of individuals of the talpid "true moles" *Talpa europaea* and *T. minor* in early Pleistocene deposits at Zabia Cave in Poland, and suggested that the cave acted as a natural trap for moles due to their burrowing activities. This might explain the abundant remains of *Na. philcreaseri* in Faunal Zone B cave deposits, without needing to assume that it was a specialised cave dweller.

A third hypothesis is that early notoryctemorphians were semi-aquatic, and that their semi-aquatic adaptations subsequently became exapted for fossoriality. Several species of talpid moles are semi-aquatic, and some authors have proposed that modern talpids all descend from a semi-aquatic ancestor (Campbell, 1939; Whidden, 1999; but see Reed 1951; Hickman 1984). Similarly, the fossorial adaptations of the living platypus (which is semi-aquatic) and echidnas (which are terrestrial) may represent exaptations from a semi-aquatic monotreme ancestor (Phillips et al., 2009; Phillips et al., 2010; Mirceta et al., 2013; but see Camens 2010; Ashwell 2013; Musser 2013). However, there is only a single extant semi-aquatic marsupial, the yapok or water-opposum *Chironectes minimus* (see Marshall, 1975; Stein and Patton, 2008), and only one questionably semi-aquatic stem-metatherian, *Didelphodon vorax* (Szalay, 1994; Longrich, 2004; but see Fox and Naylor, 2006). This suggests that marsupials are, in general, poorly adapted to semi-aquatic or aquatic niches, probably due to their reproductive mode (Lillegraven, 1975; Phillips et al., 2009). We consider it unlikely, based on available evidence, that Na. *philcreaseri* was an exception to this general rule. However, this hypothesis can be tested: Mirceta et al. (2013) showed that mammals with some degree of aquatic ancestry show elevations in myoglobin net surface charge, which is correlated with maximal skeletal muscle concentration of myoglobin, which in turn is linked with maximal active dive time underwater. Mirceta et al.'s (2013) study suggests that scalopine talpids (members of other talpid subfamilies were not sampled) and modern monotremes derive from at least semi-aquatic ancestors, but that chrysochlorids apparently do not. Using this approach, sequencing of the myoglobin locus for one or both living *Notoryctes* species should reveal whether or not they have semi-aquatic ancestry. Histological analysis of humeral microanatomy, specifically bone compactness, may also indicate whether or not *Na. philcreaseri* was semi-aquatic (Canoville and Laurin, 2010). However, a recent study of bone compactness in the humeri of talpids found no significant difference between fossorial and semi-aquatic taxa (Meier et al., 2013).

The point estimates for the age of *Na. philcreaseri* (19.4 Ma) and the timing of the *Naraboryctes-Notoryctes* split (30.3 Ma) imply that *Na. philcreaseri* post-dates the divergence between the *Naraboryctes* and *Notoryctes* lineages. However, when 95% HPDs are taken into account, these estimates overlap. In addition, the 95% HPD for the effective branch length leading to *Naraboryctes* encompasses a zero length branch. Collectively, this means that the age and known morphology of *Na. philcreaseri* is compatible with its being ancestral to *Notoryctes*. Furthermore, the postcranial differences observed between *Na. philcreaseri* and the extant *Notoryctes* species (*N. typhlops* and *N. caurinus*) appear to represent further developments of morphological trends that are apparent when comparing *Na. philcreaseri* to more generalised marsupials. They can plausibly be interpreted as reflecting more extreme specialisation towards burrowing in *Notoryctes*.

Specifically, derivation of the postcranial morphology seen in the extant *Notoryctes* species, *N. typhlops* and *N. caurinus*, from a *Naraboryctes*-like ancestor would require the following major changes. In the scapula: lengthening of the "vertebral" border and modification of the coracoid and axillary angles into hook-like processes for attachment of the subscapularis and teres major muscles; lengthening of the secondary scapular spine towards the "caudal" angle; and enlargement of the scapular spine, which curves medially towards the secondary scapular spine to enclose the infraspinatus muscle within a nearly complete tube; development of a postscapular fossa, reflecting enlargement of the triceps muscle group. In the humerus: further enlargement of the deltopectoral crest; further expansion of the medial epicondyle, increasing the surface area of origin for the forearm flexor musculature; enlargement of the lateral supracondylar ridge, increasing the surface area of origin for the forearm extensors. In the ulna: further elongation of the olecranon and development of a more marked medial curvature; broadening of the trochlear notch; deepening of the radial notch. In the radius: increased concavity of the articular surfaces for the humerus and ulna at the proximal end; broadening of the distal end. In the femur: further enlargement of the greater trochanter and the head of the femur; loss of the third trochanter, probably by proximal migration and fusion with the greater trochanter; a slight proximocaudal shift in the position of the lesser trochanter, such that it is proximodistally level with and caudal to the femoral head; increased robusticity of the femoral shaft. In the tibia: increased robusticity of the tibial shaft and further enlargement of the tibial crest, particularly at its proximal end, with development of a proximal sulcus that houses an enlarged patella.

As discussed by Archer et al. (2011), the apomorphic dental morphology of extant *Notoryctes* species can also be plausibly derived from that seen in *Na. philcreaseri*, via loss of a premolar locus (P1 is tiny in *Na. philcreaseri*), complete suppression of the paracone on the upper molars (this cusp is greatly reduced and shifted labially in *Na. philcreaseri*), and loss of the talonid on the lower molars (the talonid is present but narrow in *Na. philcreaseri*). Thus, the known dental and postcranial morphology of *Na. philcreaseri* renders it a plausible model for a plesiomorphic ancestor of *Notoryctes*.

If our estimate for the timing of inactivation of *RBP3* in the *Notoryctes* lineage, 5.4 MYA (95% HPD = 4.5–6.3 MYA;

latest Miocene to earliest Pliocene), is correct, then *RBP3* was presumably functional in the early Miocene *Na. philcreaseri*. In turn, this might be an indication that *Na. philcreaseri* still retained some visual capabilities. If so, we might predict that orbit will be more obviously identifiable on the cranium of *Na. philcreaseri* than in *Notoryctes*, in which osteological evidence for the orbit is minimal (Stirling, 1891; Carlsson, 1904; Johnson and Walton, 1989); for example, the frontal process of the jugal (for attachment of the postorbital ligament) might be more strongly developed. However, testing of this hypothesis will require the discovery of additional, more complete cranial material of *Na. philcreaseri*. Archer et al. (2011) noted that the jaw and dentition of *Na. philcreaseri* seem adapted for somewhat harder food items than those of modern *Notoryctes* species which may be an indication that the fossil taxon foraged at least some of the time on the surface (particularly soft-bodied invertebrates such as insect larvae and worms being more common below ground). Based on this combined genetic and morphological evidence (and pending the discovery of more complete cranial remains that would reveal the degree of development of its orbit), we suggest that *Na. philcreaseri* probably spent a greater proportion of its time above ground than does *Notoryctes* today, which surfaces only rarely (Johnson and Walton, 1989; Benshemesh and Johnson, 2003; Dennis, 2004; Benshemesh, 2008; Benshemesh and Aplin, 2008).

The late Miocene saw the replacement of rainforest with more open woodland environments across much of Australia, in response to a general global drying and cooling trend (Martin, 2006; Black et al., 2012). This coincided with a period of extensive faunal turnover among Australian terrestrial vertebrates (Black et al., 2012), probably including major radiations of dasyurids (Krajewski et al., 2000) and macropodids (Prideaux and Warburton, 2010).This is followed by palaeobotanical evidence for a sudden increase in the abundance of grasses in the latest Miocene (~6 MYA), from 1–2% to ~35% of the total pollen count (Martin and McMinn, 1994: fig. 2). However, true grasslands did not become widespread in Australia until the middle Pliocene (Martin, 2006; Strömberg, 2011; Black et al., 2012). If our value for the timing of *RBP3* inactivation in *Notoryctes* of 5.4 MYA (95% HPD = 4.5-6.3 MYA) is correct, it is tempting to postulate that loss of *RBP3* function is causally linked to the development of more open environments – probably open sclerophyllous woodland with a grassy understory (Strömberg, 2011), rather than true grasslands – at this time. This reduction in vegetation cover would have led to strong selection pressure on the *Notoryctes* ancestor to spend minimal time on the surface (where it would be particularly vulnerable to predators), leading to relaxation of selection on *RBP3*.

Our estimate for the timing of *RBP3* inactivation in the *Notoryctes* lineage is markedly more recent than that of Springer et al. (1998), which was 18.5–24.7 MYA, and that of Emerling and Springer (2014), which was 12.23 MYA (range of 6.87–17.84 MYA). There are a number of potential explanations for this. Springer et al.'s (1998) estimate was based on the presence of three or four indels in the *RBP3* sequence of *N. typhlops*, and the assumption that indels occur in pseudogenes at a rate of 0.17/kb/Ma. This value is a weighted average calculated from four nuclear pseudogenes (none of them *RBP3*) for seven primates, five of which (*Homo*, *Pan*, *Gorilla*, *Pongo*,and *Hylobates*) were hominoids (Saitou and Ueda, 1994). Rates varied between 0.14 and 0.24/kb/Ma across the four genes examined by Saitou and Ueda (1994), but it is unclear how much additional rate variation would be observed if more genes were to be examined. Furthermore, molecular rates of evolution vary considerably within mammals (Bininda-Emonds, 2007; Welch et al., 2008), and rates are particularly slow in hominoids relative to most other mammals, including marsupials (Bininda-Emonds, 2007). Thus, the indel rate assumed by Springer et al. (1998) may be an underestimate, in which case their estimate for the timing of *RBP3* inactivation is too old.

The approach of Emerling and Springer (2014) is conceptually similar to that used here, namely using estimated values of ω and divergence times to infer the timing of gene inactivation (see Meredith et al., 2009a). However, their estimate for ω_b (0.1007–0.1385) was lower than that calculated here (0.15635), and their estimate for ω_f (0.2928–0.3355) was higher than ours (0.244). These discrepancies may be due to differences in taxon sampling: Emerling and Springer's (2014) *RBP3* sequence alignment included 13 placentals but only five marsupials, whereas our alignment comprises 23 marsupials. In addition, Emerling and Springer (2014) used empirical estimates for ω after inactivation of *RBP3* (0.9071–1.1489) based on bat sequence data, whereas our method assumes *a priori* that ω after gene inactivation is 1, and they assumed a somewhat older estimate for the divergence of *Notoryctes* from other extant marsupials (61.28 MYA; Meredith et al., 2011) versus that used here (52.2 MYA; 95% HPD: 43.6–60.7 MYA).

Conclusion

Our qualitative and quantitative analysis of the postcranial morphology of *Na. philcreaseri* indicate that it was most likely subterranean, albeit somewhat less specialised in this regard than the living species of *Notoryctes*; the fact that *RBP3* was probably functional in *Na. philcreaseri* might be an indication that vision was more important to the fossil taxon than to *Notoryctes*, which might be evidence that it spent more time on the surface than the two living marsupial mole species. Nevertheless, it appears that notoryctemorphians had already evolved specialised, probably fully subterranean, burrowing behaviour prior to the early Miocene. A single upper molar, (NTM P2815–6) from the late Oligocene Pwerte Marnte Marnte Local Fauna in the Northern Territory, probably represents a notoryctemorphian, albeit more plesiomorphic than *Na. philcreaseri* based on its larger paracone and metaconule (Murray and Megirian, 2006: 151; Beck et al., 2014). This is the only other fossil occurrence of Notoryctemorphia currently known. A fuller understanding of the evolution of notoryctemorphians, including when and why they evolved "mole-like" behaviour, will therefore require marked improvements in the Palaeogene fossil record of mammals in Australia.

Acknowledgements

We thank Laura Wilson and Rick Arena for discussion, Sharon Jansa for help with PAML, Hayley Bates for access to JMP, and Mike Lee for assistance and advice with our Bayesian phylogenetic analyses. Kenny Travouillon provided helpful information regarding the taxonomic composition of different Riversleigh sites. Financial support for this research has been provided by the National Science Foundation (via grant DEB-0743039, in collaboration with Robert Voss at the American Museum of Natural History) and the Australian Research Council (via Discovery Early Career Researcher Award DE120100957). Additional support for research at Riversleigh has come from the Australian Research Council (LP0989969, LP100200486, and DP130100197 grants to MA and SJH), the XSTRATA Community Partnership Program (North Queensland), the University of New South Wales, Phil Creaser and the CREATE Fund, the Queensland Parks and Wildlife Service, Environment Australia, the Queensland Museum, the Riversleigh Society Inc., Outback at Isa, Mount Isa City Council, and private supporters including K. and M. Pettit, E. Clark, M. Beavis, and M. Dickson. Many volunteers, staff and students of the University of New South Wales have also assisted in field work at Riversleigh. We thank Sandrine Ladevèze and the editor Erich Fitzgerald for their helpful and constructive comments that greatly improved the final draft.

References

Abello, M. A., and Candela, A. M. (2010). Postcranial skeleton of the Miocene marsupial *Palaeothentes* (Paucituberculata, Palaeothentidae): paleobiology and phylogeny. *Journal of Vertebrate Paleontology* 30: 1515–1527.

Aplin, K., and Archer, M. (1987). Recent advances in marsupial systematics with a new syncretic classification. In M. Archer (Ed.), *Possums and opossums: studies in evolution*. (pp. xv–lxxii). Sydney: Surrey Beatty and Sons and the Royal Zoological Society of New South Wales.

Archer, M. (1984). The Australian marsupial radiation. In M. Archer, and G. Clayton (Eds.), *Vertebrate zoogeography and evolution in Australasia* (pp. 633-808). Perth: Hesperian Press.

Archer, M., Arena, D. A., Bassarova, M., Beck, R. M. D., Black, K., Boles, W. E., et al. (2006). Current status of species-level representation in faunas from selected fossil localities in the Riversleigh World Heritage Area, northwestern Queensland. *Alcheringa* 31: 1-17.

Archer, M., Beck, R. M. D., Gott, M., Hand, S., Godthelp, H., and Black, K. (2011). Australia's first fossil marsupial mole (Notoryctemorphia) resolves controversies about their evolution and palaeoenvironmental origins. *Proceedings of the Royal Society B: Biological Sciences* 278: 1498-1506.

Archer, M., and Hand, S. (1984). Background to the search for Australia's oldest mammals. In M. Archer, and G. Clayton (Eds.), *Vertebrate zoogeography and evolution in Australasia*. *(Animals in space and time)* (pp. 517-565). Carlisle, Western Australia: Hesperian Press.

Archer, M., Hand, S. J., and Godthelp, H. (1994). *Riversleigh: the story of animals in ancient rainforests of inland Australia*. Sydney: Reed Books.

Archer, M., Hand, S. J., Godthelp, H., and Creaser, P. (1997). Correlation of the Cainozoic sediments of the Riversleigh World Heritage fossil property, Queensland, Australia. In J.-P. Aguilar, S. Legendre, and J. Michauz (Eds.), *Actes du Congrès BiochroM'97* (pp. 131-152). Montpellier: École Pratique des Hautes Études, Institut de Montpellier.

Arena, D. (2004). *The geological history and development of the terrain at the Riversleigh World Heritage Area during the middle Tertiary*. Ph.D. dissertation, University of New South Wales, School of Biological, Earth and Environmental Sciences, Sydney.

Arena, D. A., Black, K. H., Archer, M., Hand, S. J., Godthelp, H., and Creaser, P. (2014). Reconstructing a Miocene pitfall trap: recognition and interpretation of fossiliferous Cenozoic palaeokarst. *Sedimentary Geology* 304: 28-43.

Asher, R. J., Horovitz, I., and Sánchez-Villagra, M. R. (2004). First combined cladistic analysis of marsupial mammal interrelationships. *Molecular Phylogenetics and Evolution* 33: 240-250.

Ashwell, K. W. S. (2013). Reflections: monotreme neurobiology in context. In K. Ashwell (Ed.), *Neurobiology of monotremes: brain evolution in our distant mammalian cousins* (pp. 285-298). Collingwood, Australia: CSIRO Publishing.

Barbour, R. A. (1963). The musculature and limb plexuses of *Trichosurus vulpecula*. *Australian Journal of Zoology* 11: 488-610.

Bates, H., Travouillon, K. J., Cooke, B., Beck, R. M. D., Hand, S. J., and Archer, M. (2014). Three new Miocene species of musky rat-kangaroos (Hypsiprymnodontidae, Macropodoidea): description, phylogenetics, and paleoecology. *Journal of Vertebrate Paleontology* 34: 383-396.

Beck, R. M. D. (2008). A dated phylogeny of marsupials using a molecular supermatrix and multiple fossil constraints. *Journal of Mammalogy* 89: 175-189.

Beck, R. M. D., Godthelp, H., Weisbecker, V., Archer, M., and Hand, S. J. (2008). Australia's oldest marsupial fossils and their biogeographical implications. *PLoS ONE* 3: e1858.

Beck, R. M. D., and Lee, M. S. Y. (2014). Ancient dates or accelerated rates? Morphological clocks and the antiquity of placental mammals. *Proceedings of the Royal Society B: Biological Sciences* 281: 20141278.

Beck, R. M. D., Travouillon, K. J., Aplin, K. P., Godthelp, H., and Archer, M. (2014). The osteology and systematics of the enigmatic Australian Oligo-Miocene metatherian *Yalkaparidon* (Yalkaparidontidae; Yalkaparidontia; ?Australidelphia; Marsupialia). *Journal of Mammalian Evolution* 21: 127-172.

Benshemesh, J. (2008). Itjaritjari, *Notorytes typhlops*. In S. Van Dyck, and R. Strahan (Eds.), *The Mammals of Australia, 3rd edition* (pp. 412-413). Sydney: Reed New Holland.

Benshemesh, J., and Aplin, K. P. (2008). Kakarratul, *Notoryctes caurinus*. In S. Van Dyck, and R. Strahan (Eds.), *The Mammals of Australia, 3rd edition* (pp. 410-411). Sydney: Reed New Holland.

Benshemesh, J., and Johnson, K. (2003). Biology and conservation of marsupial moles (*Notoryctes*). In M. Jones, C. R. Dickman, and M. Archer (Eds.), *Predators with pouches: the biology of carnivorous marsupials* (pp. 464-474). Melbourne: CSIRO Publshing.

Bi, S., Wang, Y., Guan, J., Sheng, X., and Meng, J. (2014). Three new Jurassic euharamiyidan species reinforce early divergence of mammals. *Nature* 514: 579-584.

Bininda-Emonds, O. R. P. (2007). Fast genes and slow clades: comparative rates of molecular evolution in mammals. *Evolutionary Bioinformatics* 3: 59-85.

Black, K. H., Archer, M., Hand, S. J., and Godthelp, H. (2012). The rise of Australian marsupials: a synopsis of biostratigraphic, phylogenetic, palaeoecologic and palaeobiogeographic understanding. In J. A. Talent (Ed.), *Earth and Life: Global Biodiversity, Extinction Intervals and Biogeographic Perturbations Through Time* (pp. 983-1078). Dordrecht: Springer Verlag.

Bronner, G. N. (2013). Family Chrysochloridae: golden moles. In J. Kingdon, D. C. D. Happold, T. M. Butynski, M. Hoffmann, M. Happold, and J. Kalina (Eds.), *Mammals of Africa. Volume I: introductiory chapters and Afrotheria* (Vol. Volume 1, pp. 223-257). London: Bloomsbury Publishing.

Burne, R. H. (1901). A contribution to the myology and visceral anatomy of *Chlamydophorus truncatus*. *Proceedings of the Zoological Society, London*.: 104-121.

Camens, A. B. (2010). Were early Tertiary monotremes really all aquatic? Inferring paleobiology and phylogeny from a depauperate fossil record. *Proceedings of the National Academy of Sciences of the United States of America* 107: E12-E12.

Campbell, B. (1939). The shoulder anatomy of the moles. A study in phylogeny and adaptation. *American Journal of Anatomy* 64: 1-39.

Campione, N. E., and Evans, D. C. (2012). A universal scaling relationship between body mass and proximal limb bone dimensions in quadrupedal terrestrial tetrapods. *BMC Biology* 10: 60.

Canoville, A., and Laurin, M. (2010). Evolution of humeral microanatomy and lifestyle in amniotes, and some comments on palaeobiological inferences. *Biological Journal of the Linnean Society* 100: 384-406.

Carlsson, A. (1904). Zur Anatomie des Notoryctes typhlops. *Zoologische Jahrbücher. Abteilung für Anatomie und Ontogenie der Tiere* 20: 81-122.

Casinos, A., Quintana, C., and Viladiu, C. (1993). Allometry and adaptation in the long bones of a digging group of rodents (Ctenomyinae). *Zoological Journal of the Linnean Society* 107: 107-155.

Chapman, R. N. (1919). A study of the correlation of the pelvic structure and the habits of certain burrowing mammals. *American Journal of Anatomy* 25: 185-219.

Chou, H. H., Hayakawa, T., Diaz, S., Krings, M., Indriati, E., Leakey, M., et al. (2002). Inactivation of CMP-N-acetylneuraminic acid hydroxylase occurred prior to brain expansion during human evolution. *Proceedings of the National Academy of Sciences of the United States of America* 99: 11736-11741.

Cope, E. D. (1892). On the habits and affinities of the new Australian mammal, *Notoryctes typhlops*. *American Naturalist* 26: 121–128.

Coues, E. (1872). The osteology and myology of *Didelphys virginiana*. *Memoirs of the Boston Society of Natural History* 2: 41–154.

Crosby, K. (2002). A second species of the possum *Durudawiri* (Marsupialia: Miralinidae) from the early Miocene of Riversleigh, northwestern Queensland. *Alcheringa* 26: 333-340.

Crosby, K., and Archer, M. (2000). Durudawirines, a new group of phalangeroid marsupials from the Miocene of Riversleigh, northwestern Queensland. *Journal of Paleontology* 74: 327-335.

Cúneo, R., Ramezani, J., Scasso, R., Pol, D., Escapa, I., Zavattieri, A. M., et al. (2013). High-precision U–Pb geochronology and a new chronostratigraphy for the Cañadón Asfalto Basin, Chubut, central Patagonia: Implications for terrestrial faunal and floral evolution in Jurassic. *Gondwana Research* 24: 1267-1275.

Davis, D. D. (1964). The giant panda: a morphological study of evolutionary mechanisms. *Fieldiana: Zoology Memoirs* 3: 1-339.

Dennis, C. (2004). Zoology: a mole in hand. *Nature* 432: 142-143.

dos Reis, M., Donoghue, P. C. J., and Yang, Z. (2014). Neither phylogenomic nor palaeontological data support a Palaeogene origin of placental mammals. *Biology Letters* 10: 20131003.

dos Reis, M., Inoue, J., Hasegawa, M., Asher, R. J., Donoghue, P. C., and Yang, Z. (2012). Phylogenomic datasets provide both precision and accuracy in estimating the timescale of placental mammal phylogeny. *Proc Biol Sci* 279: 3491-3500.

Edwards, L. F. (1937). Morphology of the forelimb of the mole (*Scalops aquaticus*, L.) in relation to its fossorial habits. *The Ohio Journal of Science* 37: 20-41.

Elissamburu, A., and Vizcaíno, S. F. (2004). Limb proportions and adaptations in caviomorph rodents (Rodentia: Caviomorpha). *Journal of Zoology* 262: 145-159.

Emerling, C. A., and Springer, M. S. (2014). Eyes underground: Regression of visual protein networks in subterranean mammals. *Molecular Phylogenetics and Evolution* 78C: 260-270.

Evans, H. E. (1993). *Miller's anatomy of the dog.* Philadelphia: W.B. Saunders.

Farina, R. A., and Vizcaino, S. F. (1997). Allometry of the leg bones of living and extinct armadillos. *Mammalian Biology* 62: 65-70.

Fox, R. C., and Naylor, B. G. (2006). Stagodontid marsupials from the Late Cretaceous of Canada and their systematic and functional implications. *Acta Palaeontologica Polonica* 51: 13-36.

Gambaryan, P. P., and Kielan-Jaworowska, S. (1997). Sprawling *verses* parasagittal stance in multituberculate mammals. *Acta Palaeontologica Polonica* 42: 13-44.

Gasc, J. P., Jouffroy, F. K., Renous, S., and Von Blottnitz, F. (1986). Morphofunctional study of the digging system of the Namib Desert golden mole (*Eremitalpa granti nambiensis*): cinefluorographical and anatomical analysis. *Journal of Zoology, London* 208: 9-35.

Geiger, M., Forasiepi, A. M., Koyabu, D., and Sanchez-Villagra, M. R. (2014). Heterochrony and post-natal growth in mammals - an examination of growth plates in limbs. *Journal of Evolutionary Biology* 27: 98-115.

Gott, M. (1988). *A Tertiary marsupial mole (Marsupialia: Notoryctidae) from Riversleigh, northeastern Australia and its bearing on notoryctemorphian phylogenetic systematics*. Masters Thesis, School of Biological Science, University of New South Wales,

Hickman, G. C. (1984). Swimming ability of talpid moles, with particular reference to the semi-aquatic *Condylura cristata*. *Mammalia* 48: 505-513.

Hildebrand, M. (1985). Digging of quadrupeds. In M. Hildebrand, D. M. Bramble, K. F. Liem, and D. B. Wake (Eds.), *Functional vertebrate morphology* (pp. 89-109). Cambridge, Massachusetts: Belknap Press.

Hildebrand, M., and Goslow, G. E. J. (2001). *Analysis of vertebrate structure*. USA: John Wiley & Sons, Inc.

Hopkins, S. S. B., and Davis, E. B. (2009). Quantitative morphological proxies for fossoriality in small mammals. *Journal of Mammalogy* 90: 1449-1460.

Horovitz, I., Ladevèze, S., Argot, C., Macrini, T. E., Martin, T., Hooker, J. J., et al. (2008). The anatomy of *Herpetotherium* cf. *fugax* Cope, 1873, a metatherian from the Oligocene of North America. *Palaeontographica Abteilung A* 284: 109-141.

Horovitz, I., and Sánchez-Villagra, M. R. (2003). A morphological analysis of marsupial mammal higher-level phylogenetic relationships. *Cladistics* 19: 181-212.

Jansa, S. A., and Voss, R. S. (2011). Adaptive evolution of the venom-targeted vWF protein in opossums that eat pitvipers. *PLoS ONE* 6: e20997.

Johnson, K. A., and Walton, D. W. (1989). 23. Notoryctidae. In D. W. Walton, and B. J. Richardson (Eds.), *Fauna of Australia: Volume 1B Mammalia* (pp. 1-24). Canberra: AGPS.

Kim, E. B., Fang, X., Fushan, A. A., Huang, Z., Lobanov, A. V., Han, L., et al. (2011). Genome sequencing reveals insights into physiology and longevity of the naked mole rat. *Nature* 479: 223-227.

Kirsch, J. A. W. (1977). The comparative serology of Marsupialia, and a classification of marsupials. *Australian Journal of Zoology, Supplementary Series* 52: 1-152.

Krajewski, C., Wroe, S., and Westerman, M. (2000). Molecular evidence for the pattern and timing of cladogenesis in dasyurid marsupials. *Zoological Journal of the Linnean Society* 130: 375-404.

Lagaria, A., and Youlatos, D. (2006). Anatomical correlates to scratch digging in the forelimb of European ground squirrels (*Spermophilus citellus*). *Journal of Mammalogy* 87: 563-570.

Lanfear, R., Calcott, B., Ho, S. Y., and Guindon, S. (2012). Partitionfinder: combined selection of partitioning schemes and substitution models for phylogenetic analyses. *Molecular Biology and Evolution* 29: 1695-1701.

Lehmann, W. H. (1963). The forelimb architecture of some fossorial rodents. *Journal of Morphology* 113: 59-76.

Lessa, E. P. (1990). Morphological evolution of subterranean mammals: integrating structural, functional, and ecological perspectives. *Progress in Clinical and Biological Research* 335: 211-230.

Lessa, E. P., Vassallo, A. I., Verzi, D. H., and Mora, M. S. (2008). Evolution of morphological adaptations for digging in living and extinct ctenomyid and octodontid rodents. *Biological Journal of the Linnean Society* 95: 267-283.

Lewis, P. O. (2001). A likelihood approach to estimating phylogeny from discrete morphological character data. *Systematic Biology* 50: 913-925.

Lillegraven, J. A. (1975). Biological considerations of the marsupial-placental dichotomy. *Evolution* 29: 707-722.

Longrich, N. (2004). Aquatic specialization in mammals from the Late Cretaceous of North America. *Journal of Vertebrate Paleontology* 24: 84A.

MacAlister, A. (1875a). Report on the anatomy of the insectivorous edentates. *Transactions of the Royal Irish Academy* 24: 491-508.

Macalister, M. B. (1875b). A monograph of the anatomy of *Chlamydophorus Truncatus* (Harlan) with notes on the structure of other species of Edentata. *Transactions of the Royal Irish Academy* 25: 219-278.

Marshall, L. G. (1975). *Chironectes minimus*. *Mammalian Species* 109: 1-6.

Martin, H. A. (2006). Cenozoic climatic change and the development of the arid vegetation in Australia. *Journal of Arid Environments* 66: 533-563.

Martin, H. A., and McMinn, A. (1994). Late Cainozoic vegetation history of north-western Australia from the palynology of a deep sea core (ODP site 765). *Australian Journal of Botany* 42: 95-102.

McLaren, S., and Wallace, M. W. (2010). Plio-Pleistocene climate change and the onset of aridity in southeastern Australia. *Global and Planetary Change* 71: 55-72.

Meier, P. S., Bickelmann, C., Scheyer, T. M., Koyabu, D., and Sanchez-Villagra, M. R. (2013). Evolution of bone compactness in extant and extinct moles (Talpidae): exploring humeral microstructure in small fossorial mammals. *BMC Evolutionary Biology* 13: 55.

Meredith, R. W., Gatesy, J., Murphy, W. J., Ryder, O. A., and Springer, M. S. (2009a). Molecular decay of the tooth gene enamelin (*ENAM*) mirrors the loss of enamel in the fossil record of placental mammals. *PLoS Genetics* 5: e1000634.

Meredith, R. W., Janecka, J. E., Gatesy, J., Ryder, O. A., Fisher, C. A., Teeling, E. C., et al. (2011). Impacts of the Cretaceous Terrestrial Revolution and KPg extinction on mammal diversification. *Science* 334: 521-524.

Meredith, R. W., Krajewski, C., Westerman, M., and Springer, M. S. (2009b). Relationships and divergence times among the orders and families of Marsupialia. *Museum of Northern Arizona Bulletin* 65: 383-406.

Meredith, R. W., Westerman, M., Case, J. A., and Springer, M. S. (2008). A phylogeny and timescale for marsupial evolution based on sequences for five nuclear genes. *Journal of Mammalian Evolution* 15: 1-36.

Milne, N., and O'Higgins, P. (2012). Scaling of form and function in the xenarthran femur: a 100-fold increase in body mass is mitigated by repositioning of the third trochanter. *Proceedings of the Royal Society B: Biological Sciences* 279: 3449-3456.

Mirceta, S., Signore, A. V., Burns, J. M., Cossins, A. R., Campbell, K. L., and Berenbrink, M. (2013). Evolution of mammalian diving capacity traced by myoglobin net surface charge. *Science* 340: 1234192.

Mitchell, K. J., Pratt, R. C., Watson, L. N., Gibb, G. C., Llamas, B., Kasper, M., et al. (2014). Molecular phylogeny, biogeography, and habitat preference evolution of marsupials. *Molecular Biology and Evolution*.

Muirhead, J. (1997). Two new early Miocene thylacines from Riversleigh, northwestern Queensland. *Memoirs of the Queensland Museum* 41: 367-377.

Murray, P. F., and Megirian, D. (2006). The Pwerte Marnte Marnte Local Fauna: a new vertebrate assemblage of presumed Oligocene age from the Northern Territory of Australia. *Alcheringa* Special Issue 1: 211-228.

Musser, A. M. (2013). Classification and evolution of the monotremes. In K. Ashwell (Ed.), *Neurobiology of monotremes: brain evolution in our distant mammalian cousins* (pp. 1-16). Collingwood, Australia: CSIRO Publishing.

Nevo, E. (1979). Adaptive convergence and divergence of subterranean mammals. *Annual Review of Ecology and Systematics* 10: 269-308.

Nevo, E. (1999). *Mosaic evolution of subterranean mammals: regression, progression and global convergence*. Oxford: Oxford University Press.

Nilsson, M. A., Arnason, U., Spencer, P. B. S., and Janke, A. (2004). Marsupial relationships and a timeline for marsupial radiation in South Gondwana. *Gene* 340: 189–196.

Nilsson, M. A., Churakov, G., Sommer, M., Tran, N. V., Zemann, A., Brosius, J., et al. (2010). Tracking marsupial evolution using archaic genomic retroposon insertions. *PLoS Biology* 8: e1000436.

Orcutt, E. E. (1940). Studies on the muscles of the head, neck, and pectoral appendages of *Geomys bursarius*. *Journal of Mammalogy* 21: 37-52.

Pepperberg, D. R., Okajima, T. L., Wiggert, B., Ripps, H., Crouch, R. K., and Chader, G. J. (1993). Interphotoreceptor retinoid-binding protein (IRBP). Molecular biology and physiological role in the visual cycle of rhodopsin. *Molecular Neurobiology* 7: 61-85.

Phillips, M. J., Bennett, T. H., and Lee, M. S. Y. (2009). Molecules, morphology, and ecology indicate a recent, amphibious ancestry for echidnas. *Proceedings of the National Academy of Sciences of the United States of America* 106: 17089-17094.

Phillips, M. J., Bennett, T. H., and Lee, M. S. Y. (2010). Reply to Camens: How recently did modern monotremes diversify? *Proceedings of the National Academy of Sciences of the United States of America* 107: E13-E13.

Prideaux, G. J., and Warburton, N. M. (2010). An osteology-based appraisal of the phylogeny and evolution of kangaroos and wallabies (Macropodidae: Marsupialia). *Zoological Journal of the Linnean Society* 159: 954-987.

Puttick, G. M., and Jarvis, J. U. M. (1977). The functional anatomy of the neck and forelimbs of the Cape Golden Mole, *Chrysochloris asiatica* (Lipotyphla: Chrysochloridae). *Zoologica Africana* 12: 445-458.

Reed, C. A. (1951). Locomotion and appendicular anatomy in three soricoid insectivores. *American Midland Naturalist* 45: 513-665.

Ronquist, F., Klopfstein, S., Vilhelmsen, L., Schulmeister, S., Murray, D. L., and Rasnitsyn, A. P. (2012a). A total-evidence approach to dating with fossils, applied to the early radiation of the Hymenoptera. *Systematic Biology* 61: 973-999.

Ronquist, F., Teslenko, M., van der Mark, P., Ayres, D. L., Darling, A., Hohna, S., et al. (2012b). MrBayes 3.2: efficient Bayesian phylogenetic inference and model choice across a large model space. *Systematic Biology* 61: 539-542.

Rose, K. D., and Emry, R. J. (1983). Extraordinary fossorial adaptations in the Oligocene palaeanodonts *Epoicotherium* and *Xenocranium* (Mammalia). *Journal of Morphology* 175: 33-56.

Rougier, G. W., Martinelli, A. G., Forasiepi, A. M., and Novacek, M. J. (2007). New Jurassic mammals from Patagonia, Argentina: a reappraisal of australosphenidan morphology and interrelationships. *American Museum Novitates* 3566: 1-54.

Rzebik-Kowalska, B. (2013). *Sorex bifidus* n. sp. and the rich insectivore mammal fauna (Erinaceomorpha, Soricomorpha, Mammalia) from the Early Pleistocene of Żabia Cave in Poland. *Palaeontologia Electronica* 16: 12A.

Saitou, N., and Ueda, S. (1994). Evolutionary rates of insertion and deletion in noncoding nucleotide sequences of primates. *Molecular Biology and Evolution* 11: 504-512.

Salton, J. A., and Sargis, E. J. (2008). Evolutionary morphology of the Tenrecoidea (Mammalia) forelimb skeleton. In E. J. Sargis, and M. Dagosto (Eds.), *Mammalian Evolutionary Morphology: A Tribute to Frederick S. Szalay* (pp. 51-72). Dordrecht, The Netherlands: Springer.

Schaller, O. (Ed.). (1992). *Illustrated veterinary anatomical nomenclature*. Stuttgart: Enke.

Shen, B., Fang, T., Dai, M., Jones, G., and Zhang, S. (2013). Independent losses of visual perception genes *Gja10* and *Rbp3* in echolocating bats (Order: Chiroptera). *PLoS ONE* 8: e68867.

Springer, M. S., Burk, A., Kavanagh, J. R., Waddell, V. G., and Stanhope, M. J. (1997). The interphotoreceptor retinoid binding protein gene in therian mammals: implications for higher level relationships and evidence for loss of function in the marsupial mole. *Proceedings of the National Academy of Sciences of the United States of America* 94: 13754-13759.

Springer, M. S., Westerman, M., Kavanagh, J. R., Burk, A., Woodburne, M. O., Kao, D. J., et al. (1998). The origin of the Australasian marsupial fauna and the phylogenetic affinities of the enigmatic monito del monte and marsupial mole. *Proceedings of the Royal Society B Biological Sciences* 265: 2381-2386.

Stein, B. R. (1986). Comparative limb myology of four arvicolid rodent genera (Mammalia; Rodentia). *Journal of Morphology* 187: 321-342.

Stein, B. R. (1993). Comparative hindlimb morphology in geomyine and thomomyine pocket gophers. *Journal of Mammalogy* 74: 86-94.

Stein, B. R., and Patton, J. L. (2008). Genus *Chironectes* Illiger, 1811. In A. L. Gardner (Ed.), *Mammals of South America. Vol. 1. Marsupials, xenarthrans, shrews, and bats* (pp. 14-17). Chicago: Chicago University Press.

Stirling, E. C. (1888). Preliminary notes on a new Australian mammal. *Transactions of the Royal Society of South Australia* 11: 21-24.

Stirling, E. C. (1891). Description of a new genus and species of Marsupialia, *Notoryctes typhlops*. *Transactions of the Royal Society of South Australia* 14: 154-187.

Strömberg, C. A. E. (2011). Evolution of grasses and grassland ecosystems. *Annual Review of Earth and Planetary Sciences* 39: 517-544.

Sweet, G. (1906). Contribution to our knowledge of the anatomy of *Notoryctes typhlops*, Stirling. Part III - the eye. *Quarterly Journal of Microscopical Science* 50: 547-572.

Szalay, F. S. (1994). *Evolutionary history of the marsupials and an analysis of osteological characters*. Cambridge: Cambridge University Press.

Szalay, F. S., and Sargis, E. J. (2001). Model-based analysis of postcranial osteology of marsupials from the Palaeocene of Itaboraí (Brazil) and the phylogenetics and biogeography of Metatheria. *Geodiversitas* 23: 139-302.

Taylor, B. K. (1978). The anatomy of the forelimb of the anteater (*Tamandua*) and its functional implications. *Journal of Morphology* 157: 347-368.

Thompson, P., and Hillier, W. T. (1905). The myology of the hindlimb of the marsupial mole (*Notoryctes typhlops*). *Journal of Anatomy and Physiology* 34: 308-331.

Thorington, R. W. J., Darrow, K., and Betts, A. D. K. (1997). Comparative myology of the forelimb of squirrels (Sciuridae). *Journal of Morphology* 234: 155-182.

Travouillon, K. J., Archer, M., Hand, S. J., and Godthelp, H. (2006). Multivariate analyses of Cenozoic mammalian faunas from Riversleigh, northwestern Queensland. *Alcheringa* Special Issue 1: Proceedings of CAVEPS 2005: 323-349.

Travouillon, K. J., Legendre, S., Archer, M., and Hand, S. J. (2009). Palaeoecological analyses of Riversleigh's Oligo-Miocene sites: implications for Oligo-Miocene climate change in Australia. *Palaeogeography, Palaeoclimatology, Palaeoecology* 276: 24-37.

Turnbull, W. D. (1971). The Trinity therians: their bearing on evolution in marsupials and other therians. In A. A. Dahlberg (Ed.), *Dental morphology and evolution* (pp. 151-179). Chicago: University of Chicago Press.

Turnbull, W. D., and Reed, C. A. (1967). *Pseudochrysochloris*, a specialized burrowing mammal from the early Oligocene of Wyoming. *Journal of Paleontology* 41: 623-631.

Vassallo, A. I. (1998). Functional morphology, comparative behaviour, and adaptation in two sympatric subterranean rodents genus *Ctenomys* (Caviomorpha: Octodontidae). *Journal of Zoology* 244: 415-427.

Vizcaino, S. F., Farina, R. A., and Mazzetta, G. V. (1999). Ulnar dimensions and fossoriality in armadillos. *Acta Theriologica* 44: 309-320.

Vizcaino, S. F., and Milne, N. (2002). Structure and function in armadillo limbs (Mammalia : Xenarthra : Dasypodidae). *Journal of Zoology* 257: 117-127.

Warburton, N. M. (2003). *Functional morphology and evolution of marsupial moles (Marsupialia; Notoryctemorphia)*. Unpublished Ph.D. dissertation, University of Western Australia,

Warburton, N. M. (2006). Functional morphology of marsupial moles (Marsupialia, Notoryctidae). *Verhandlungen des Naturwissenschaftlichen Vereins in Hamburg* 42: 39-149.

Warburton, N. M., Gregoire, L., Jacques, S., and Flandrin, C. (2013). Adaptations for digging in the forelimb muscle anatomy of the southern brown bandicoot (*Isoodon obesulus*) and bilby (*Macrotis lagotis*). *Australian Journal of Zoology* 61: 402-419.

Welch, J. J., Bininda-Emonds, O. R., and Bromham, L. (2008). Correlates of substitution rate variation in mammalian protein-coding sequences. *BMC Evolutionary Biology* 8: 53.

Whidden, H. P. (1999). The evolution of locomotor specializations in moles. *American Zoologist* 39: 135A.

Windle, B. C. A., and Parsons, F. G. (1899). On the myology of the Edentata. *Proceedings of the Zoological Society, London* 67: 314-339.

Woodhead, J., Hand, S. J., Archer, M., Graham, I., Sniderman, K., Arena, D. A., et al. (2014). Developing a radiometrically-dated chronologic sequence for Neogene biotic change in Australia, from the Riversleigh World Heritage Area of Queensland. *Gondwana Research*.

Woodman, N., and Gaffney, S. A. (2014). Can they dig it? Functional morphology and semifossoriality among small-eared shrews, genus *Cryptotis* (Mammalia, Soricidae). *Journal of Morphology* 275: 745-759.

Yang, Z. (2007). PAML 4: phylogenetic analysis by maximum likelihood. *Molecular Biology and Evolution* 24: 1586-1591.

Zhang, Z. D., Cayting, P., Weinstock, G., and Gerstein, M. (2008). Analysis of nuclear receptor pseudogenes in vertebrates: how the silent tell their stories. *Molecular Biology and Evolution* 25: 131-143.